



Exploring Iso-mukaadial acetates and other small compounds as inhibitors of recombinant *Plasmodium falciparum* lactate dehydrogenase

A dissertation submitted in fulfilment of the requirements for the degree of Masters of Medical Science in Medical Biochemistry

School of Laboratory Medicine and Medical Sciences

Discipline of Medical Biochemistry

University of KwaZulu-Natal

By

Nonduduzo Hlengiwe Mabaso

(217015953)

Supervisor: Dr Ndumiso N. Mhlongo

Co-Supervisor: Dr Ofentse J. Poee

2021

Declaration

I, Nonduduzo Hlengiwe Mabaso (217015953), declare that this dissertation titled “Exploring Iso-mukaadial acetates and other small compounds as inhibitors of recombinant *Plasmodium falciparum* lactate dehydrogenase”, submitted to the University of KwaZulu-Natal for Master of Medical Sciences under the school of Laboratory Medicine and Medical Sciences has not been submitted to any other University. This is completely the results of my own work, and anything that is not my work has been referenced in an appropriate manner. I understand that plagiarism is a serious offence, hence, I have faithfully acknowledged all the sources used.

Signature:

Date: 30 November 2021

Acknowledgements

All thanks go to God first for giving me the strength to write and be able to complete my research project. It is also my greatest desire to acknowledge the following individuals, who have been with me from the beginning till the end. These people have played a huge role and were very potent for the completion of my Msc degree. I first want to acknowledge my supervisors Dr Mhlongo and Dr Poee for the opportunity they have both given me to pursue this research project. I am also grateful for the support and guidance they have shown me. I also want to acknowledge National Research Foundation (NRF) for funding my research project.

Furthermore, I would also want to show my sincere gratitude to the School of Laboratory Medicine and Medical Sciences for granting me an opportunity to do my Msc research project and my family, for all their support and prayers. Finally, my co-postgraduate students who were with me daily in the laboratory; Lindiwe Zuma, Xolani Mazibuko, Thando Gasa and Avanthi Moodley for the support they have shown me.

Dedication

I dedicate this dissertation to the Almighty God and my parents, Mr and Mrs Mabaso.

Contents

Declaration	ii
Acknowledgements	iii
Dedication	iv
List of symbols and abbreviations	vii
List of tables	ix
List of Figures	ix
Abstract	1
Chapter 1: INTRODUCTION	2
Chapter 2: LITERATURE REVIEW	5
CHAPTER 2	5
2.1 Overview of malaria	5
2.2 The malaria parasite life cycle.....	7
2.3 Lactate dehydrogenases	8
2.4 <i>Plasmodium falciparum</i> lactate dehydrogenase (PfLDH) significance in parasite metabolism	9
2.5 Malaria diagnosis using parasite PfLDH	9
2.6 Role of <i>Plasmodium falciparum</i> lactate dehydrogenase in parasite cycle	10
2.7 <i>P. falciparum</i> and other parasites drug resistance	11
2.8 <i>P. falciparum</i> mechanism of resistance	13
2.9 Anti-malarial drug resistance and <i>Plasmodium</i> parasites that developed drug resistance	14
2.10 Traditional herbal compounds (Traditional medicine)	14
2.11 Newly discovered compounds	16
Research focus	18
CHAPTER 3: Materials and Methods	19
3.1 Chemicals and Reagents	19
3.2 Double Digestion for conformation of gene inside Pkk223 plasmid/ Agarose gel electrophoresis .	19
3.3 Colony PCR and agarose gel electrophoresis for insert confirmation.	20
3.4 Protein expression of recombinant PfLDH.....	20
3.5 Purification of expressed PfLDH protein.....	21
3.6 Determination of PfLDH protein concentration with Bradford assay	21
3.7 Interaction Studies: Fourier transform infrared (FTIR) analysis and Ultraviolet-visible spectroscopy (UV-Vis)	22
3.8 Thermal stability assay.....	22

3.9 Computational studies.....	23
3.10 <i>Plasmodium falciparum</i> compound inhibition studies.	24
CHAPTER 4: Results AND Discussion.....	25
4.1 Colony PCR, Recombinant pKK223/PfLDH expression and purification	25
4.2 Interaction Studies: Fourier transform infrared (FTIR) analysis and Ultraviolet-visible spectroscopy (UV-Vis)	27
4.3 Thermal stability assay.....	30
4.4 Molecular docking.....	31
Below is a table representing docking scores, type of interaction, distance, and binding affinity between PfLDH and the four investigated compounds (IMA, BA, UA, OEA) with the standard chloroquine. It also shows 2D and 3D figures representing the interaction of the compounds with the PfLDH protein.....	31
4.5 <i>Plasmodium falciparum</i> PfLDH inhibition studies.....	35
CHAPTER 5: Conclusion.....	39
References.....	40

List of symbols and abbreviations

Abbreviations	Symbol interpretation
PfLDH	<i>Plasmodium falciparum</i> lactate dehydrogenase
3D	Three dimensional
BC	Before Christ
AD	After Christ
CQ	Chloroquine
ACT	Artemisinin- based combination therapy
PfDHPS	<i>Plasmodium falciparum</i> Dihydropteroate synthetase
PfDHFR	<i>Plasmodium falciparum</i> Dihydrofolate reductase
IMA	Iso-mukaadial acetate
BA	Betulinic acid
UA	Ursolic acid
OEA	Oleanolic acid
ATP	Adenosine triphosphate
DNA	Deoxyribonucleic acid
RNA	Ribonucleic acid
TCA	Tricarboxylic acid cycle (Krebs cycle)
SDS-PAGE	Sodium dodecyl sulphate- Polyacrylamide gel electrophoresis
UV-Vis	Ultraviolet-visible spectroscopy
FTIR	Fourier transform infrared

BSA	Bovine serum albumin
IC ₅₀	Inhibitory concentration
WB	<i>Warburgia salutaris</i>
WHO	World health organization
NADH	Nicotinamide adenine dinucleotide
EUM	<i>Eucomis autumnalis</i>
PCR	Polymerase chain reaction

List of tables

Table 1: Antimalarial derivatives that have develop resistance along the years.....	12
Table 2: Docking scores (kcal/mol) and types of protein-ligand interactions for the binding mode of Iso-makaadial acetate, Betulinic acid, Ursolic acid, Oleanolic acid and Chloroquine ligands with PfLDH.....	31
Table 3: IC ₅₀ values for the screened compounds against asexual <i>Plasmodium falciparum</i> parasite, using SYBR Green I based assay.....	37

List of Figures

Figure 1: Map displaying parts of the world where malaria is dominant.....	6
Figure 2: The lifecycle of malaria parasite in the mosquito vector and human host.....	7
Figure 3: glycolytic pathway step showing simultaneous inter-conversion of pyruvate to lactate and nicotinamide adenine dinucleotide (NAD)H to NAD ⁺	8
Figure 4: On-bead PfLDH activity assay.....	10
Figure 5: Biochemical drug- resistance mechanisms found in parasite. These steps demonstrate possible ways that could lead to <i>P. falciparum</i> being resistance to drugs.....	13
Figure 6: Structure of the Isolated Compounds; iso-mukaadial acetate, Betulinic Acid, Ursolic Acid and Oleanolic Acid.....	16
Figure 7: PKK223 plasmid map and Agarose gel electrophoresis of PCR products generated by colony PCR.....	25
Figure 8: SDS-PAGE showing expression and purification of PfLDH in 2YT medium at 25°C and western blot showing purification of Recombinant PfLDH.....	26
Figure 9: Uv-vis absorption spectra of PfLDH in the presence of Iso-mukaadial acetate, Betulinic acid, Ursolic acid and Oleanolic acid.....	27
Figure 10: FTIR spectra of PfLDH-compound interaction.....	29
Figure 11: Thermal shift assay using cy5-5 environmentally sensitive fluorophores to check PfLDH stability in the presence of a compound.....	30

Figure 12: Three (3D) structure and two- dimensional (2D) structure of Chloroquine.....	33
Figure 13: Three (3D) structure and two- dimensional (2D) structure of Ursolic acid.....	33
Figure 14: Three (3D) structure and two- dimensional (2D) structure of Iso-mukaadial acetate (A), Betulinic acid (B).....	34
Figure 15: Three (3D) structure and two- dimensional (2D) structure of Oleanolic acid.....	35
Figure 16: Dose response curves for the compounds and extracts tested for antimalarial activity.....	38

Abstract

Malaria is a major killer disease in Sub-Saharan Africa, this disease is caused by a protozoan parasite of genus *Plasmodium*. It is a pressing health issue the public is facing, and the effectiveness of every treatment developed thus far is being jeopardized by the emergence of parasite drug resistance. This then creates a demand for new antiprotozoal medication, necessitating novel approaches that will assure the long-term discovery of the lead compounds. The investigation of compounds such as Iso-mukaadial acetate (IMA), Betulinic acid (BA), Ursolic acid (UA) and Oleanolic acid (OEA) which are isolated from plants shows to possess antimalarial activity. These compounds either originate from various plants or leaves, IMA which is isolated from a pepper bark tree, BA from bark of a plant species (white birch), UA from leaves of (lavender, rosemary), and OEA found in leaves and *Olea europaea* fruit. This study aims to investigate the inhibitory properties of these compounds against *Plasmodium falciparum* lactate dehydrogenase (PFLDH) an enzyme found in the parasite glycolytic pathway that converts pyruvate to lactate and in so doing, provides the energy needed for the survival of the malarial parasite. These methodologies were followed to conduct this study; Recombinant PFLDH was expressed and then purified for further analysis including colony PCR, expression, purification, interaction studies including Fourier transform infrared (FTIR) analysis and Ultraviolet-visible spectroscopy (UV-Vis), antimicrobial activity along with *in silico* analysis. The following results were obtained: Colony PCR confirmed the presence of a 951bp insert in the PKK223 plasmid. Metal affinity chromatography successfully purified PFLDH protein sized 34.9kDa which was confirmed by ExPasy ProtParam server. The following results were obtained from isolated compounds (BA and IMA) that were screened for IC₅₀ to demonstrate overall activity against the asexual *P. falciparum*. BA and IMA had IC₅₀ values of 1.27 and 1.03µg/ml against asexual *P. falciparum*, respectively. When compounds were incubated with protein, FTIR analysis showed a clear shift in the curve, which is indicative of an interaction between IMA and BA with PFLDH. UV-Vis showed that structural conformational change was induced, resulting in an interaction of the compounds with the aromatic side chains of PFLDH. The *in silico* analysis showed where these interactions occurred, highlighting the ligand atoms responsible for the interaction. Based on these findings, it is possible that these investigated compounds could be effective PFLDH inhibitors as they have binding affinities which are like the standard drug, chloroquine (QA).

Keywords: Malaria, Plasmodium falciparum, Compounds, Interaction studies, *in silico* analysis.

Chapter 1: INTRODUCTION

1.1 Introduction

Protozoal infections have a huge impact on people's health (primarily in the tropical and subtropical areas), the economy and society. They have a significant contribution to the global burden of infectious disease at large. Some of the serious disease that threaten almost one-sixth of the world population are Malaria (*Plasmodium* species), various forms of cutaneous and visceral leishmaniasis (*Leishmania* species), amoebic dysentery (*Entamoeba* species), African sleeping sickness (*Trypanosoma cruzi*) and toxoplasmosis (*Toxoplasma* species)(Capela et al., 2019). Ecological modifications and environmental changes caused by natural and human-caused events have had and will continue having a significant impact on the emergence and the spread of these infections (Capela et al., 2019). Some of these environmental changes includes climate change, ozone depletion, loss of biodiversity, changes in hydrological system and freshwater supplies, land degradation and urbanization. These are among the environmental threats to human health at the global and regional level, according to the World Health Organization (Nava et al., 2017).

Limited availability of effective vaccinations for the prevention and treatment of human protozoan infections has amplified the diseases impact. Unfortunately, the effectiveness of currently available treatment (chloroquine) for malaria is being jeopardized by the emergence of parasite drug resistance. Therefore the demand for new antiprotozoal medication propels research around the world, necessitating novel approaches that will assure the long-term discovery of lead compounds (Capela et al., 2019). Protozoa, which is a causative agent of malaria is a single-celled microscopic organism found all over the world. Over 65,000 of these species have been identified, and they are described as organisms that consist of a complicated internal structure and engage in very complicated metabolic activities (Capela et al., 2019). The protozoa complicated internal structure along with complicated metabolic activities is contributing to this organism being able to hide or develop ways of being resistance to the existing drugs such as chloroquine. This study is investigating indigenous medicinal plants *Warburgia salutaris* (stem bark) and *Eucomis autumnalis* (bulbs) as potential inhibitors of *P. falciparum* proteins implicated in malaria. It is also

investigating four isolated compounds: Iso-mukaadial acetate, Betulinic acid, Ursolic acid and Oleanolic Acid as potential inhibitors of recombinant *Plasmodium falciparum* lactate dehydrogenase (PfLDH).

1.2 Structure of the Thesis

1. Chapter 1: General introduction and presentation of research problem.
2. Chapter 2: Overview of malarial, parasite life cycle and role of PfLDH / Drug discovery and resistance
4. Chapter 3: Methods and materials
5. Chapter 4: Presentation of results and discussion
6. Chapter 5: Conclusion and Future perspective

Chapter 2: LITERATURE REVIEW

CHAPTER 2

2.1 Overview of malaria

Plasmodium falciparum is the most common *Plasmodium* species that causes malaria. This disease is passed on to humans by a female infected mosquito known as anopheles species (Wang et al., 2017). A study done by the World Health Organization, reveals that malaria continues to be a critical issue in developing countries, with over 200 million cases and nearly 450,000 deaths in 2017 mostly in African sub-Saharan countries. These numbers are evidence that this disease requires our most serious attention (Opoku et al., 2019). The high temperatures in the tropical and subtropical regions enables this disease to be passed on easily as the mosquito thrives in these conditions. (Keiser et al., 2005). There are five *Plasmodium* parasites out of a hundred that have a potential to infect humans. The *P. vivax* parasite being most dominant in South America and Asia while *P.falciparum* remains a serious issue in Sub-Saharan Africa countries (Sementa Khuzwayo Biochemistry, 2019). A short erythrocyte cycle of *P. falciparum* is what results in many merozoites which are released to invade further red blood cells. This further invasion could be associated with the loss of human red blood cells and possible anemia. The erythrocytic stage of the malaria infection, in which the parasite undergoes continuous intracellular growth, leading to exponential parasite proliferation, is exclusively associated with the morbidity and mortality rate reported of the disease. This condition might potentially lead to serious implications including kidney disease, mental instability and possibly death if left unattended (Mathema & Na-Bangchang, 2015).

Inhibiting the PfLDH protein may result in the death of *P. falciparum*. As a result, PfLDH and the glycolysis pathway are excellent targets for drug development (Mathema & Na-Bangchang, 2015). A good diagnostic marker that could be used to predict the efficiency of the antimalarial drug would be Histidine-rich protein 2 (HRP-2), as this is a unique protein produced by *Plasmodium falciparum*, this means if the drug has been effective in clearing the infection this protein should not be found in the bloodstream (Sementa Khuzwayo Biochemistry, 2019).

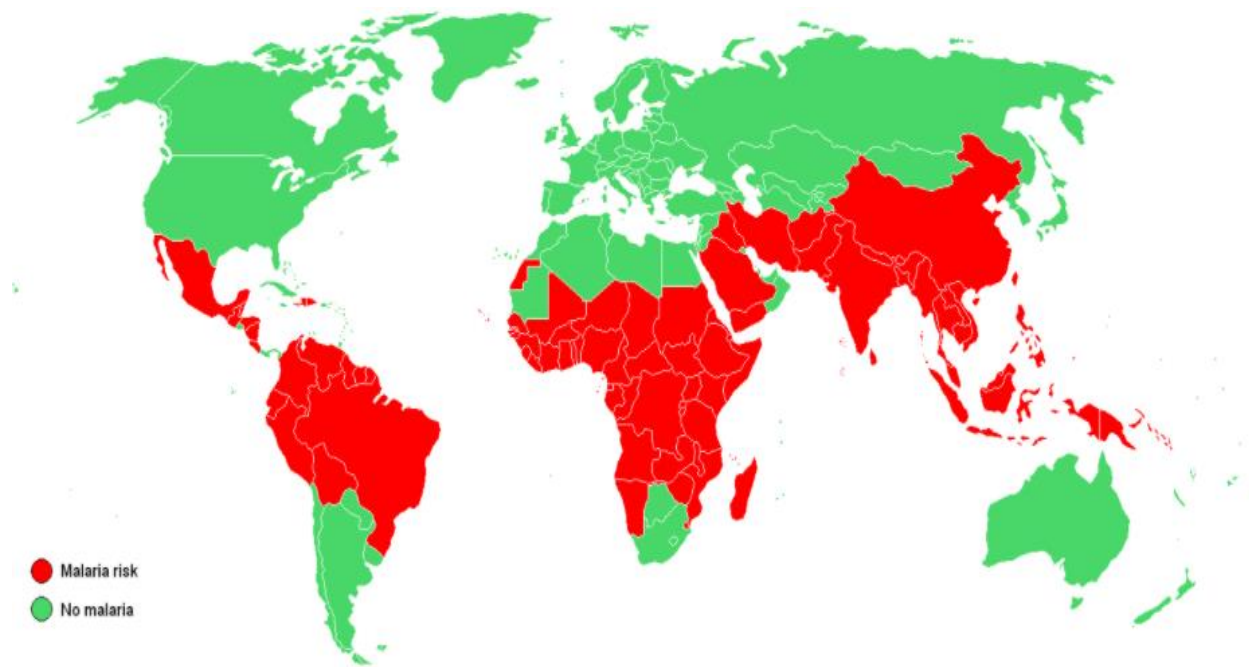


Figure 1: Map displaying parts of the world where malaria is dominant (File: Malaria map.PNG,2020).

Plasmodium species have two life stages: sexual (mosquito vector) and asexual (Homo sapiens) Talapko et al., 1999). The parasite has evolved several strategies to assist it in evading the human immune system, making the parasite familiar to the treatment resulting in its efficiency being highly reduced (Alam et al., 2014; Hyde, 2007). The figure that follows is a malaria lifecycle showing how the parasite is transmitted from a vector (mosquito) to the host (Homo sapiens).

2.2 The malaria parasite life cycle

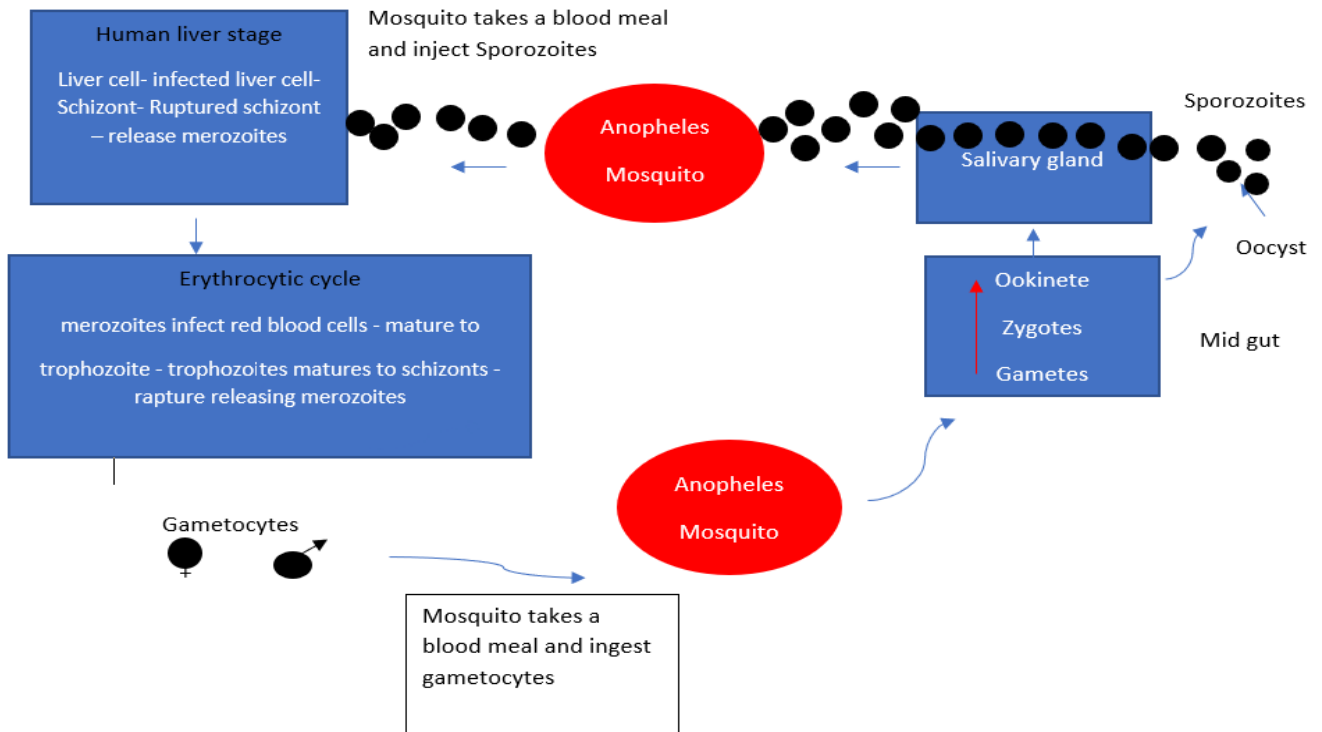


Figure 2: The lifecycle of malaria parasite in the mosquito vector and human host. During blood feeding, the *Anopheles* mosquito releases sporozoites. These sporozoites infect the liver cells (hepatocytes), where they develop and infect red blood cells. The asexual stage results in the development of schizonts, which infect more red blood cells and in the production of gametocytes, which are consumed by the mosquito during blood feeding on the infected person. Inside the mosquito (midgut), the gametes transform into zygotes, which eventually form the Ookinete. The Ookinete develops into an Oocyst, which contains sporozoites. These are then released into the mosquito's salivary gland in preparation for the next blood meal (<https://www.malariasite.com/life-cycle/>).

2.3 Lactate dehydrogenases

Dehydrogenases are a class of biological catalysts involved in oxidoreduction reactions discovered by T. Turnberg between 1900 and 1922. These enzymes are found in human tissues, plants as well as certain microorganisms. They are also classified as oxidoreductase and known to possess multiple subunits given that it is a multienzyme complex. This is a tetrameric enzyme composed of two subunits: the M subunit (also known as LDHA) found in skeletal muscle as well as the H subunit (also known as LDHB) located in the heart. It also acts as a 2-hydroxy acid oxidoreductase accelerating the conversion of pyruvate to lactate and nicotinamide adenine dinucleotide (NAD)H to NAD⁺ (Valvona et al., 2015). The figure below is a representation of how pyruvate is converted to lactate.

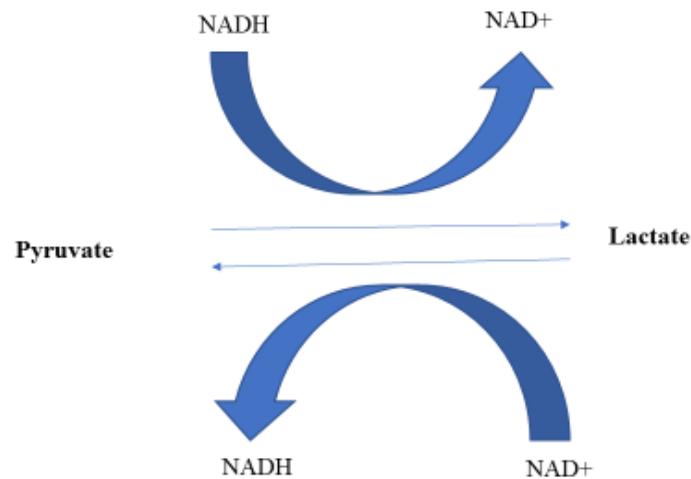


Figure 3: glycolytic pathway step showing simultaneous inter-conversion of pyruvate to lactate and nicotinamide adenine dinucleotide (NAD)H to NAD⁺

2.4 *Plasmodium falciparum* lactate dehydrogenase (PfLDH) significance in parasite metabolism

Plasmodium falciparum relies greatly on the enzyme PfLDH. Besides its importance in the production of energy and the consequent survival of *P. falciparum*, PfLDH also facilitates the conversion of pyruvate to lactate in the final reaction of glycolysis. The cells of *P. falciparum* are unable to fully generate ATP via their citric acid cycle, consequentially PfLDH provides a valuable alternative to enable energy production. Given the key role of PfLDH in the survival of *P. falciparum*, this enzyme may be investigated as a potential target for the discovery and development of drugs to hinder this human malaria parasite (Pradhan et al., 2009). The development of such an anti-malarial drug may require screening of analogs of NADH, an important PfLDH cofactor. Continuous efforts to discover and investigate new drug target molecules have been active since the early introduction of quinolones used in the treatment of malaria. One such example is that of CQ, which has been shown to act as a competitive inhibitor through interactions with the NADH binding pockets of PfLDH. (Nwazue, 2012). Similar examples have indicated the ability of other drugs to target LDH, albeit in cancer cells. Such cancer cells display a metabolic preference for glycolysis instead of oxidative phosphorylation even when exposed to high oxygen concentrations. A further study discovered inhibition of LDHA by 1-(phenylseleno)-4-(trifluoromethyl)benzene thereby highlighting its potential as an anti-tumour drug.

2.5 Malaria diagnosis using parasite PfLDH

For years the detection of the malaria parasite has relied largely on the use of PfLDH. This enzyme assay relies on the ability of PfLDH to make use of 3-acetylpyridine dinucleotide (APAD) as an alternative to NADH. In this case, APAD acts as the coenzyme required to enable the formation of lactate from pyruvate. However, in the presence of APAD human red blood cells, LDH performs this reaction at a much slower rate. A study conducted in Kenya has shown that a newer enzymatic assay, which makes use of parasite LDH to diagnose LDH, displays greater sensitivity and specificity when compared to microscopy, thereby enabling the detection of parasites that may not be visualized by microscopy (Nwazue, 2012). An alternative assay, the magnetic bead-based colorimetric assay, may also be applied for the detection of PfLDH. The assay relies on the

extraction of a specific biomarker in the blood of the parasite, followed by the addition of an α -PfLDH magnetic bead which are anti-*P. falciparum* LDH antibody. The magnetic bead binds to the PfLDH (as it is a PfLDH antibody raised in mouse using *Plasmodium falciparum* conjugated to HRP as the immunogen, this making it specific to PfLDH) and enables the consequent magnetic separation of the bound PfLDH and the remaining non-specific proteins. Buffer is used to wash the separated PfLDH after which the enzymatic activity may be assessed through an optimised colorimetric enzyme reaction. This simple assay offers a highly effective technique for the detection of *P. falciparum* and the associated diagnosis of malaria (Markwalter et al., 2016).

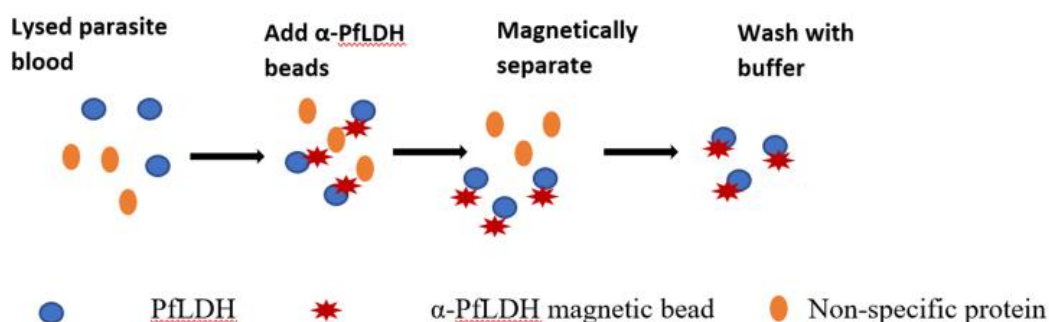


Figure 4: On-bead PfLDH activity assay (Markwalter et al., 2016)

2.6 Role of *Plasmodium falciparum* lactate dehydrogenase in parasite cycle

The pathogen appears to rely on lactate dehydrogenase as its critical enzyme in the glycolytic pathway to transform pyruvate into lactate during the intraerythrocytic stages of the parasite's life cycle. This is because the enzymes involved in energy metabolism lack a functional TCA, and development of ATP is entirely dependent on the glycolytic pathway among other enzymes. It can be said that this pathway is therefore critical for the parasite's survival, so any inhibition of the PfLDH protein could result in *P. falciparum*'s death. This then makes PfLDH and the glycolysis pathway good target for drug design as inhibition of PfLDH results in parasite death within cultured red blood cells. Since the PfLDH differs significantly from the human type of the enzyme in terms of structure, this biomarker has the potential to be used to develop promising antimalarial drug targets or diagnostic methods (Mathema & Na-bangchang, 2015). Despite significant progress

in malaria control over the last decade, it remains a major public health issue around the world. The continued rise in antimalarial drug resistance has necessitated the development of novel antimalarial drugs (Opoku et al., 2019).

2.7 *P. falciparum* and other parasites drug resistance

Antimalarial drug resistance is defined as a *Plasmodium* parasite strain's ability to survive and continuously proliferate despite the administration of equal or higher drug dose than usually recommended. To discover resistant malaria parasite and measure their level of resistance, researchers used two fundamental methods: *in vitro* and *in vivo*. Although *in vitro* techniques are highly recommended for demonstrating biological resistance to antimalarials, *in vivo* results or clinical response to therapy are frequently difficult to accommodate. This was proven in the following; *P. falciparum* isolates obtained in Kenya showed *in vitro* chloroquine resistance of 8% while *in vivo* tests conducted in the same areas of Kenya over the same period revealed parasitological failure rates of more than 80% and clinical failure rates of more than 50% (Barat & Bloland, 1997).

Chloroquine proved to be effective against all human species (*P. vivax*, *P. falciparum*, *P. ovale*, and *P. malariae*), regardless of where the person contracted the disease (Barat & Bloland, 1997). Malaria was initially treated with quinine containing Cinchona tree in America in 1934. To alleviate symptoms related to malaria like fever, Quinghaosu (Artemisinin) the Chinese herb was administered. Hans Andersag, a German disclosed Resochin in 1934 which was then termed Chloroquine (CQ) following World War II in 1946. In Asia, around 1960s and 1970s Chloroquine lost its potency against *P. falciparum* malaria as the parasite manifest genetically mediated chloroquine resistance (Eugene, 2017). CQ resistance caused worldwide declines in the attempts to stop malaria. This caused malaria to emerge again and CQ resistant parasite to escalate in southern Asia and South America. The spread of the CQ resistant parasite also escalated to Africa in 1980 with 2-3 folds increase in deaths owing to the lack of suitable drugs for treating malaria. There was then a return of CQ with sulfadoxine/ pyrimethamine (SP), which also became ineffective due to parasite resistance causing wide spread of malaria. (Antony and Parija, 2016). Different reasons might have contributed to this drug resistance. Artemisinin-based combination

therapy was used instead of monotherapy to increase drug potency and prevent drug resistance parasite. However, drug resistance to these parasites have also been reported in Southern Asia (Antony and Parija, 2016). This concept has caused an urgency for malaria vaccines including parasites divergence. Although complexity of *Plasmodium* presents difficulties in the design of new vaccines it also brings about chances to develop new vaccines. One of the opportunity this complexity presents is that it poses many targets antigens for incorporation into different therapeutic. Both traditional and bioinformatic ways assist in the development of vaccines and understanding pathogenesis (Vaughan et al., 2010).

Table 1: Antimalarial derivatives that have develop resistance along the years.

Antimalarial derivatives	Drug name	Mechanism of action	Resistance status
1. Quinoline derivatives	Chloroquine	➤ Accumulate in digestive vacuole of parasite	Yes
	Amodiaquine		
	Quinine		
	Mefloquine		
	Halofantrine	➤ heme detoxification inhibition	
	Lumefantrine		
	Primaquine	➤ Not known	Yes
	Atovaquone	➤ Inhibits parasite respiratory reaction	Yes
2. Antifolate derivatives	Slulfadoxine, Sulfene	➤ PfdHPS inhibition ➤ Inhibition of folate biosynthesis	Yes
	Pyrimethamine, Proguanil	➤ Inhibits PfdHFR activity ➤ Inhibition of folate biosynthesis	Yes
3. Artemisinin derivatives	Artesunate	➤ Not known	Yes

2.8 *P. falciparum* mechanism of resistance

Like living organisms, parasites are capable of evading antimalarial drug action. They do this through a variety of complex biochemical pathways. The mechanism of drug resistance proceeds in this manner; drug action can be prevented by cells hiding in sanctuary locations, adjusting drug uptake mechanisms, or changing membrane composition, this all-hinder drug uptake. Drugs may either be inactivated, expelled, chemically changed with the intention to ease excretion, or being directed into compartments away from the target site once within the parasite. Mechanisms of drug activation could be lost or inhibited by raising the number of competing substrate or modifying the target to make it less responsive to the drug and making the drug's interaction with the target less effective. Finally, by bypassing the block, the cell may learn to live with a blocked target (Ouellette & Ward, 2003). The figure below shows all the possible scenarios that leads to *P. falciparum* drug resistance.

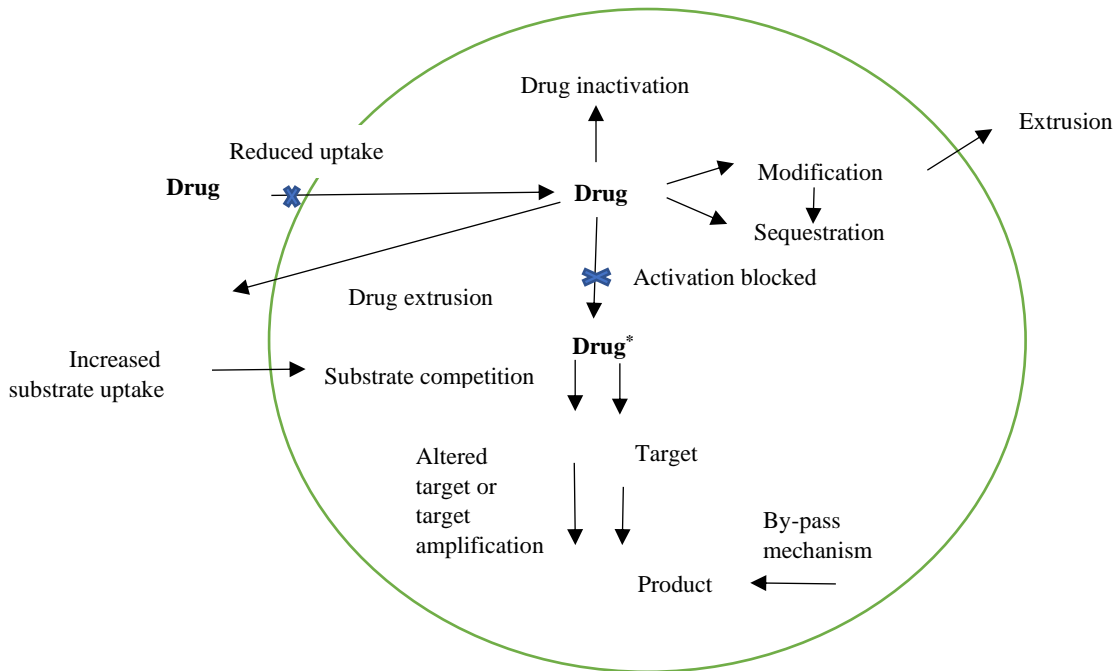


Figure 5: Biochemical drug- resistance mechanisms found in parasite. These steps demonstrate possible ways that could lead to *P. falciparum* being resistance to drugs.

2.9 Anti-malarial drug resistance and *Plasmodium* parasites that developed drug resistance

There are four important terminologies in malaria resistance, these terms are recurrence, recrudescence, relapse, and resistance (4R's). Asexual parasitemia can reoccur after therapy or after a fresh infection. The recurrence of asexual parasitemia of the same infection after treatment of the original sickness is known as recrudescence. Asexual parasitemia caused by lingering liver stages from persisting hypnozoites causes relapse in *P. vivax* and *P. ovale* malaria. The ability of a parasite to be able to survive and also reproduce despite adequate dosage is known as resistance (Resistance, 2020). Malaria has over 200 million cases with 435,000 deaths estimated worldwide in the year 2017, more importantly 70% of the malaria estimated cases and death globally were contributed by 11 countries (Sub-Saharan Africa and India contributing 10 out of the 11 countries). Out of all four human species of malaria, *Plasmodium falciparum* and *Plasmodium vivax* are the parasites that cause the most instances and the most severe illnesses, as well as the most drug-resistant infections (Capela et al., 2019). There are a handful factors that contributes to the appearance of resistance to existing antimalarial drugs such as, the parasite mutation rate, the strength of drug selected, overall parasite load, the treatment compliance and failure in following malaria treatment guidelines (Resistance, 2020).

2.10 Traditional herbal compounds (Traditional medicine)

For over 1,000 years, traditional medicines have been used to treat malaria, and two major categories of antimalarial drugs are derived from them (artemisinin and quinine derivatives). On top of the issue poor people are facing in terms of not affording effective drugs for malaria treatment and rising drug resistance, traditional medicines could be a potential and sustainable source of treatment (Willcox & Bodeker, 2004). Through ethnobotanical studies, it has been predicted that 122 medications from 94 plant species have already been found; an example is the herbal 'Qing Hao Su' which is extracted from a medicinal plant and is used as an antipyretic and wormwood in parts of China (Fabricant & Farnsworth, 2001). Use of medicinal plants had a very significant role in most rural area ensuring daily health care of people. In some ethnic groups of Southern Cameroon, traditional medicine is more popular and used more often compared to western medicine (Pierre et al., 2011).

Secondary metabolites in medicinal plants have biological activities as well as several plant-derived compounds (Opoku et al, 2019). The development of new antimalarials is required, and research primary method have been to use various approaches, such as testing natural products and synthetic molecules (Wang et al, 2017). A lot of malaria treatment historically comes from plants and about 80 percent of rural African population depend on or view traditional medicine as a source of treatment to treat diseases, such as malaria. To some rural African people traditional medicine is not only a form of treatment but using traditional medicine is also viewed as connecting to your identity and following in the foots of your ancestors as an African person. *Warburgia salutaris* (pepper- bark tree) is a traditional medicine found in Southern African region, with properties of being ever-green and the ability to grow up to 10 meters in height. This pepper- bark tree has been used for the treatment of chest infections, ulcers, and bronchitis. The tablet form of *W.salutaris* have been used as a natural antibiotics which acts against oral thrush. The roots and leaves of the bark tree are being validated scientifically as use of malaria treatment in traditional medicine. A study was conducted with an aim to validate the use of *W. salutaris* as Zulu traditional medicine scientifically. This study began with the extraction of stem bark, followed by column chromatography which finally led to the isolation of iso-mukaadial acetate compound. The compound was spectroscopically analyzed by hydrogen and carbon NMR. MTT assay measured cytotoxicity on HEK293 and HEPG2 cell lines. *In vivo* studies show that *W. salutaris* crude extract and iso-mukaadial acetate were orally taken by Chloroquine-sensitive *Plasmodium berghei* infected rats, this was followed by percentage parasitaemia and haematological parameters determination. Results showed that *W. salutaris* possess anti- malarial activity, and its traditionally shown to treat malaria however more studies are still required to test its mechanism of action. (Nyaba Z. N et al, 2018). On the other hand, Betulinic acid is a naturally occurring chemical present in a variety of plants, as well as in the *Ziziphus* species with antioxidant activity and medicinal properties such as pain relief, chest pains, eye infection and diarrhea. It has also been shown to possess biological and therapeutic activity such as anticancer, antimicrobial, anti-inflammatory, and antimalarial (Nyaba et al., 2018; Wang et al., 2017).

Although traditional medicine is frequently used to treat malaria and typically more accessible and less expensive than Western treatment. However, it does have limitations. To begin with, clinical evidence on safety and efficacy are scarce. Second, even among traditional healers, there is no agreement on which plants, preparations, or dosages are the most beneficial. Finally, depending

on a variety of conditions, the concentration of active chemicals in a plant species varies greatly. Regardless of these limitation, this could be resolvable through research as Research Initiative on Traditional Antimalarial Methods has published systematic reviews as well as guidelines with the aim of standardizing and improving future research quality (Willcox & Bodeker, 2004).

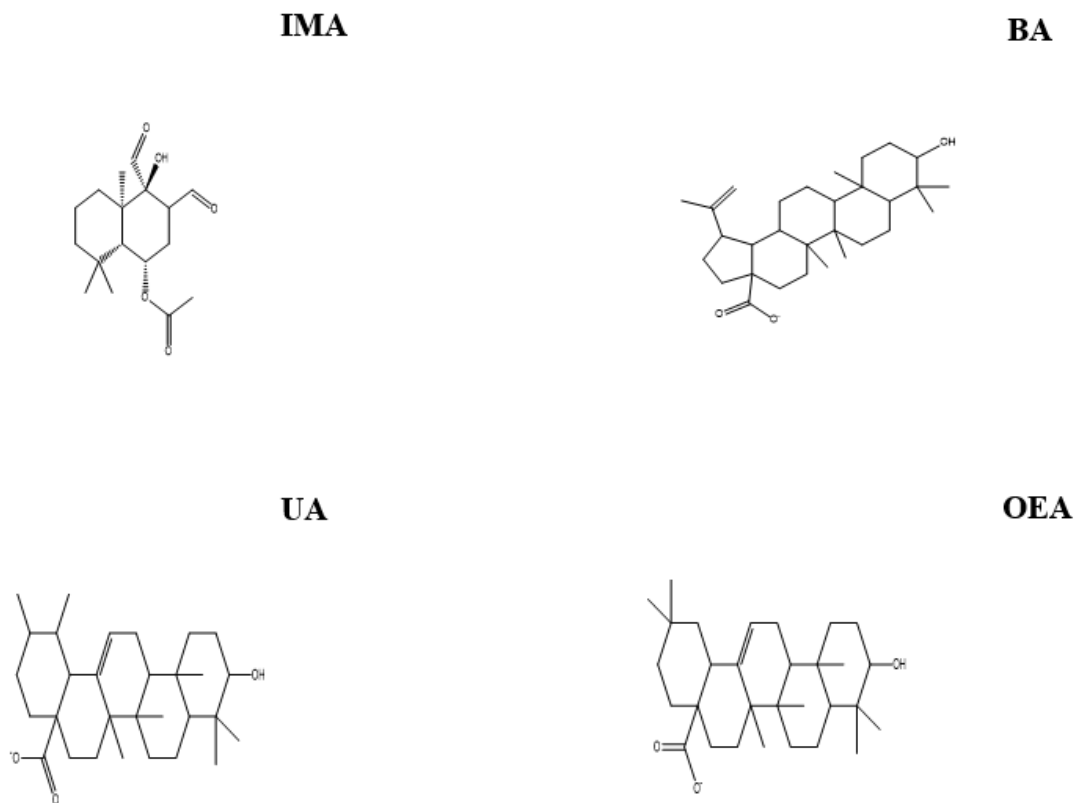


Figure 6: Structure of the Isolated Compounds; iso-mukaadial acetate (IMA), Betulinic Acid (BA), Ursolic Acid (UA) and Oleanolic Acid (OEA)

2.11 Newly discovered compounds

From the past some of the compounds used for the malarial treatment therapy includes, Quinine, Mepacrine, Chloroquine, Mefloquine and Halofantrine. The world health organization has pointed out 14 medicines for malaria treatment and 4 medicines as preventative treatment, which could either be a single compound or a combination compound. The present compounds used for malaria treatment are Artemisinin and its derivatives. Artemisinin was isolated from a herb used in China

traditional medicine called *Artemisia annua* in the year 1971. Some of the Artemisinin derivatives are artemether, and artesunate. All the present multidrug-resistance variants of *Plasmodium falciparum* have shown to be susceptible to artemisinin. Using artemisinin has been critical in fighting malaria, and artemisinin combination therapy accounts for most of the present treatment. Western Cambodia reported its first resistance case in the year 2008 to artemisinin, then in the year 2018 there was a report identifying a number of artemisinin resistance cases in Southeast Asia. The other present compounds are Amodiaquine, Piperaquine, Lumefantrine, Pyronaridine, Pyrimethamine & sulfadoxine and Tafenoquine to name a few. For future malaria treatment, the potential of a compounds to be a new anti-malarial is judged by a few requirements: a compound should possess a novel mode of action with no cross-resistance to present drugs, should cure in a single dose and should have activity against asexual blood stage causing malaria and gametocyte which are responsible for the transmission of the disease. Exploring new combinations may assist with overcoming resistance against malaria but alternatively using existing medications that have been used for other purpose may be found effective against malarial treatment. This could be beneficial as these compounds may have already demonstrated good biological characteristics and potentially reveal novel mechanism of action. Some of these compounds could be Methylene blue which is a methaemoglobinemia therapy medication. Another compound is an anti-diabetic medication called rosiglitazone, which is currently being tested as therapy for severe malaria. Imatinib is an anti-cancer medication, and as a triple composition with dihydroartemisinin-piperaquine (Tse et al., 2019).

Research focus

Problem statement:

The effectiveness of currently available treatment for malaria is being jeopardized by the emergence of parasite drug resistance, therefore the demand for new antiprotozoal medication propels research around the world.

Aim:

Aim of this study is to investigate Iso-mukaadial acetate (IMA), Betulinic acid (BA), Ursolic acid (UA) and Oleanolic Acid (OEA) inhibition against *Plasmodium falciparum* lactate dehydrogenase (malaria protein) and determine the mechanism of action of these four compounds in in vitro models.

Specific objectives:

- To do a colony PCR to confirm presence of an insert which is 951 bp in the Pkk223 plasmid.
- To perform an expression and purification of Recombinant PfLDH
- To confirm expression and purification of PfLDH protein using Western blot analysis.
- To perform a Fourier, transform infrared (TFIR) analysis and Ultraviolet-visible spectroscopy (UV-Vis) to investigate the interaction of Iso-mukaadial acetate (IMA), Belutinic acid (BA), Ursolic acid (UA) and Oleanolic acid (OEA) with PfLDH protein.
- To perform thermal stability assay, to find out if the four investigated compounds improve thermal stability of PfLDH protein.
- To perform computational studies to observe where the direct interaction between the compounds and PfLDH occur.
- Finally perform anti-malarial assay using NF54 (drug sensitive) strain of *P. falciparum* parasites to confirm if these compounds are antimalarial. (This was outsourced from the Malaria Parasite Molecular Laboratory (M²PL).

CHAPTER 3: Materials and Methods

This chapter summaries the major methodology conducted in this study to reach a conclusion.

3.1 Chemicals and Reagents

The reagents used in this research work were purchased from Sigma-Aldrich (South Africa), LTC tech (Gauteng, South Africa), Bio-Rad Laboratories Inc. (Johannesburg, South Africa), ThermoFisher scientific (Johannesburg, South Africa), and Yaksha (Durban, South Africa). The reagents include: agar, sodium chloride, yeast extract, tryptone, peptone, glycerol, potassium dihydrogen phosphate (KH_2PO_4), dipotassium phosphate (K_2HPO_4), Ampicillin, bacterial protein extraction reagent (B-PER), Isopropyl β -D-1-thiogalactopyranoside (IPTG), 40% bis- acrylamide, 1.5 tris (pH8.8), 10% sodium dodecyl sulphate (SDS), 10% ammonium persulphate (APS), N,N,N',N'-tetramethylethylenediamine (TEMED), 0.5 tris (pH 8.8), sodium dihydrogen phosphate monohydrate ($\text{NaH}_2\text{PO}_4 \cdot \text{H}_2\text{O}$), imidazole, tris buffered saline (TBS), tris buffered saline with Tween 20 detergent (TBST), skimmed milk, monoclonal Anti-polyHistidine-Peroxidase antibody, 3,3',5,5'- tetramethylbenzidine (TMB), dimethylsulfoxide (DMSO), bromophenol blue, ethidium bromide, , bovine serum albumin (BSA), coomassie brilliant blue G-250, cy5-5 environmentally sensitive fluorophore .

3.2 Double Digestion for conformation of gene inside Pkk223 plasmid/ Agarose gel electrophoresis

After performing a DNA extraction using DNA extraction kits (Zymo research Corp; California, USA), to obtain the DNA, a double digestion was performed to conform the presence of a recombinant gene encoding PflDH inside the Pkk223 plasmid. Four micro-centrifuge tubes each consisting of a final volume of 20 μl were used. All the tubes (appendix C) were incubated for 1 hour at 37 °C to be run on an 1 % agarose gel electrophoresis.

1% Agarose gel and sample preparations

0.5 g of agarose was weighed and 50 ml 1 \times TAE buffer was added and heated until agarose was dissolved. The mixture was then allowed to cool down before the addition of 5 μl Ethidium bromide. The mixture was then poured on to the tray and allowed to set. The tubes in the incubator were each added with 3 μl loading dye and a marker was prepared by adding 3 μl loading dye to

3 μ l lambda DNA cut with HindIII. Prepared samples were loaded on the gel and run at 100 V for 40 minutes to be viewed on a Gel documentation imager.

3.3 Colony PCR and agarose gel electrophoresis for insert confirmation.

To confirm presence of an insert in PKK223 plasmid, Colony PCR was conducted where, a forward primer of length 21 base pairs, sequenced 5'ATGGCACCAAAAGCAAAAATC3' and with a T_m min/max of 48.5, and a reverse primer of length 22 base pairs, sequenced 5'TTAAGCTAATGCCTTCATTCTC3' and with a T_m min/max of 49.25 were used for PflDH amplification using colony polymerase chain reaction (PCR). First colonies were grown in a streak plate where an inoculum was diluted by streaking it an agar plate surface. colony PCR was conducted by picking one colony and transferring it to a tube with forward/ reverse primer (Inqaba biotech; Gauteng, South Africa), Taq polymerase (Inqaba biotech; Gauteng, South Africa) and sterile water (this serving as a PCR reaction tube) done in duplicates. The second tube was a no template control tube, consisting of primers and Taq polymerase but omitting DNA to serve as a control for nucleic acid contamination. Inqaba biotechnology protocol was used for the preparation of primers and settings of the annealing temperature on the PCR machine with the following PCR conditions in appendix D. After colony PCR the samples were prepared to be loaded and run in an agarose gel electrophoresis (prepared using the same protocol as the one above).

3.4 Protein expression of recombinant PflDH

PflDH gene (obtained in PlasmODB, a biological database for the genus *Plasmodium*) encoding histidine sequence was ligated into pKK223 vector which was then transformed into and expressed in E. coli BL21 (DE3) cells. To confirm the expression and how much protein the cell expressed per hour, the cells were cultured in a 2YT medium (see preparation of medium in appendix B) and incubated at 25 °C with 160 rpm shaker until an OD of 0.4 was reached. Isopropyl β -d-1-thiogalactopyranoside (IPTG), at a final concentration of 1 mM was then added and incubation was continued at 25 °C with a shaker at 160 rpm and OD readings were taken at 6, 12, 24,36 and 48 hours. After taking each OD reading cells were centrifuge at 6200 \times g for 4 minutes, then resuspended in Bacterial Protein Extraction Reagent B-PER (thermo scientific; Johannesburg,

South Africa). Recombinant protein expression was then confirmed by running a 12 % Sodium dodecyl sulfate-polyacrylamide gel electrophoresis (SDS-PAGE) (gel preparation in appendix E) and validated with western blot following a standard procedure, using a monoclonal Anti-polyHistidine-Peroxidase antibody produced in mouse in a working dilution of 1:2000 (Lueangyangyuen et al., 2021).

3.5 Purification of expressed PflLDH protein

The expressed protein was purified with immobilized metal affinity chromatography (IMAC) using Ni-NTA (nickel-nitrilotriacetic acid) Sepharose. The bacterial cells were pellet by centrifugation at 3500×g for 30 minutes, then the pellet was resuspended in B-PER reagents. This was followed by incubation at 25° C to allow the cells to lyse then another centrifugation at 3500×g for 30 minutes. The obtained supernatant was incubated with the Ni-NTA affinity column at 4°C for 1 h, then washed with 25 ml of LEW buffer followed by the second wash with 10ml LEW buffer (20 mM NaH₂PO₄.H₂O, mM NaCl, and 100 mM imidazole) to effectively remove nonspecific bindings before the His tagged recombinant protein was eluted with elution buffer (20 mM NaH₂PO₄.H₂O, mM NaCl, and 500 mM imidazole). A 12% SDS-PAGE and Western blot analysis were done to analyze and confirm PflLDH purity (Lueangyangyuen et al., 2021; Salomane et al., 2021).

3.6 Determination of PflLDH protein concentration with Bradford assay

The purified PflLDH protein concentration was determined by Bradford assay, where bovine serum albumen (BSA) standard was prepared into concentration ranging from 0-100 µg/ml (0,6.25, 12.5, 25, 50, 100 µg/ml) in 0.15 M NaCl. Addition of 1.5 ml Bradford reagents to BSA followed by incubation at room temperature in a dark room for 10 minutes. Absorbance was read at 595 nm using a spectrophotometer then the absorbance values and the BSA concentration were used to plot the standard curve (appendix G). To measure the purified PflLDH, 1.5ml Bradford reagent was added to 10µl of PflLDH protein and 90µl of NaCl then incubated in a dark room at 25°C for 10 minutes. Absorbance was read at 595 nm then using the equation the concentration of PflLDH was

calculated. Taking into account of a dilution factor the answer was multiplied by 10 to get the actual protein concentration.

3.7 Interaction Studies: Fourier transform infrared (FTIR) analysis and Ultraviolet-visible spectroscopy (UV-Vis)

The purified 382.14 μ g/ml P_fLDH protein was incubated with 5mM IMA, BA, UA and OEA which were prepared in dimethyl sulfoxide (DMSO). The protein-ligand complex between the compounds and the P_fLDH was allowed to form by incubating for 1 hour at 25°C. The FTIR measurements were done at 25°C using IRAffinity-1S where a background scan of purification buffer was done before reading of samples. The sample readings were done for P_fLDH only and in solution with IMA, BA, UA and OEA. The IR spectral shift readings, which are the vibration frequencies in the amide band A, B, I, III and III were determined between 400 – 4000 cm⁻¹ at a resolution of 4 cm⁻¹ with 32 scans. OriginPro 8.5 software was used to analyze the FTIR spectral data and to deconvolute the amide band I region for P_fLDH secondary motif structures using the Fit-Peak Pro option (Salomane et al., 2021). To Further understand the protein-ligand interaction, UV-Vis spectrometer analysis was performed. This technique was to monitor the secondary structural conformational changes through three aromatic amino acid: Phenylalanine, Tyrosine and Tryptophan induced by the four compounds (IMA, BA, UA and OEA). P_fLDH was exposed for 15 minutes to 0.05, 0.5 and 5mM IMA, BA, UA and OEA at room temperature, the spectral analysis was done before and after addition of compounds. The spectra were normalized, and the correction of baseline was done with OriginPro8.5 software followed with the smoothing and cleaning up of the data set (Opoku et al., 2019).

3.8 Thermal stability assay

The principle of thermal shift assay is that a protein can be thermally stabilized by the presence of a ligand, leading to a higher apparent melting temperature. Bio-Rad protein thermal shift protocol was used to conduct a thermal stability assay where 382.14 μ g/ml P_fLDH protein was incubated with 5 mM, 0.5 mM and 0.05 Mm of IMA, BA, UA and OEA which were prepared in dimethyl sulfoxide (DMSO). P_fLDH and compounds were added in real-time PCR plate, followed by

addition of 1µl cy5 and cy5-5 environmentally sensitive fluorophores and Tris/HCL buffer to make up to a total volume of 25µl. Thermal unfolding was monitored from 10 °C to 95 °C at 0.5 °C interval. The final step was the analysis of the thermal melting profiles (Shift & Preparation, n.d.).

3.9 Computational studies

Molecular docking

Molecular docking was conducted with an aim to research the computational binding affinities between PflLDH and four compounds (IMA, BA, UA and OEA). Molecular docking involves three main steps, which are: 1) obtaining protein crystal structure and compound structure, 2) Protein/ligand preparation, 3) Docking process. The PflLDH crystal structure with ID 1T2D, resolution 1.10 Å was retrieved from Protein Data Bank (<https://www.wwpdb.org/>) and saved as a PDB format whereas the compounds structures were obtained from PubChem (<https://pubchem.ncbi.nlm.nih.gov>). The PflLDH protein was prepared by MOE 2015.10 (<https://www.macinchem.org/reviews/moe2015.php>) where the preparation involved removal of water molecules, followed by the addition of polar hydrogen, and assigning types for all atoms. The following step was fixing the protein structure by removing the other ligands originally bound to the crystal structure but leaving the ligand (NAD). The 3D crystal structure was then protonated. The final step of protein preparation was the isolation of active site, where site finder was applied, and backbone atoms were isolated. IMA, BA, UA, and OEA structures were retrieved from Pubchem and then added to MOE 2015.10, where further preparations were done. Ligand's preparation involved protonating 3D structure and adding partial charges, this was followed by potential energy and energy minimization of the four ligand structures. The prepared ligand structures were saved in MOE format and were ready for docking. This was then followed by the actual docking process where prepared PflLDH protein was docked with prepared IMA, BA, UA, OEA and Chloroquine which was used as a standard using MOE 2015.10 server (Ajmal Ali, 2020; K. Ambre et al., 2013).

3.10 *Plasmodium falciparum* compound inhibition studies.

Finally, the SYBR Green I based assay was employed to test the ant- plasmodial activity of the four compounds (IMA, BA, UA and OEA) and to determine the inhibitory concentration of these compounds. The assay was conducted using the drug sensitive *P. falciparum* strain, NF54 (Maboane & Maboane, 2021). This assay further enabled the quantitative measurement of the IC₅₀ values of the compounds: IMA, BA, UA and OEA with the aim of investigating the extent of activity if these compounds against the *P. falciparum* parasites. The parasites were kept at 37°C in a suspension of human red blood cells (O+) in complete culture medium [RPMI 1640 medium (Sigma-Aldrich) supplemented with 25 mM HEPES (Sigma-Aldrich), 20 mM D-glucose (Sigma-Aldrich), 200 µM hypoxanthine (SigmaAldrich), 0.2% sodium bicarbonate, 24 µg/ml Gentamycin (Sigma-Aldrich) and 0.5% AlbuMAX II] in a gaseous environment of 90% N₂, 5% O₂, and 5% CO₂ as described. The in vitro, ring-stage, intra-erythrocytic parasite cultures (drug sensitive, NF54 strain, genotyped) (200 µl at 1% haematocrit, 1% parasitaemia) were analysed along with the extracts. Chloroquine disulphate (1 µM, as positive control) and complete RPMI media (negative control) as well as grown over 96 hours at 37°C under the 90% N₂, 5% O₂, and 5%CO₂ gas mixture in 96-well plates, were applied as controls in this assay. Following this 96-hour growth time, equal volumes (100 µl each) of the *P. falciparum* parasite cultures were mixed with SYBR Green I lysis buffer (0.2 µl/ml 10 000xSYBR Green I, Invitrogen; 20 mM Tris, pH 7.5; 5 mM EDTA; 0.008% (w/v) saponin; 0.08% (v/v) Triton X-100). Thereafter, samples were incubated for 1 hour at 37°C. The GloMax®-Multi+ Detection System with Instinct® Software (Promega, excitation at 485 nm and emission at 538 nm) was used to facilitate quantification of sample fluorescence. To determine an accurate measure of *P. falciparum* proliferation, the background fluorescence (i.e., that measured in the samples derived from chloroquine-treated red blood cells samples in which parasite proliferation was completely inhibited) was subtracted from each sample total fluorescence. The resulting data was investigated using Excel and by plotting associated sigmoidal dose-response curves in GraphPad 8.0. It should be noted that all experiments were repeated n=3 times (Maboane & Maboane, 2021).

CHAPTER 4: Results AND Discussion

4.1 Colony PCR, Recombinant pKK223/PfLDH expression and purification

The colony PCR successfully confirmed the presence of an insert with size 951bp in Pkk223 plasmid (figure 7b).

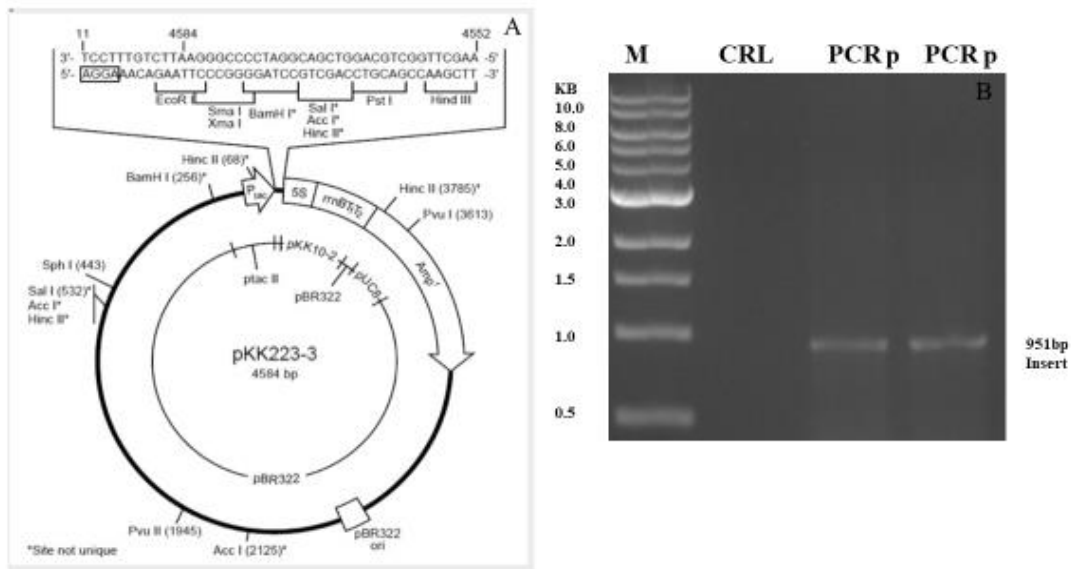


Figure 7: PKK223 plasmid map (A) and Agarose gel electrophoresis of PCR products generated by colony PCR (B) lane M: marker, lane CRL: no template control, lane PCR p: PCR products. Three tubes were prepared, two of which were the reaction tubes containing reverse and forward primers, Taq polymerase and colonies (DNA). The other tube served as a no template control, containing forward and reverse primers, Taq polymerase and omits DNA template from a reaction to serve as a general control for external nucleic acid contamination. This colony PCR was done to confirm presence of an insert which is 951bp in the Pkk223 plasmid.

To conclude that the gene encoding PfLDH was successfully cloned in the plasmid or to validate that it was a correct gene we require an additional step which is performing sequencing. Affinity purification visualized by 12.5% SDS-PAGE and confirmation of the expression and purification by western blot (figure 8) using a monoclonal Anti-polyHistidine-Peroxidase antibody.

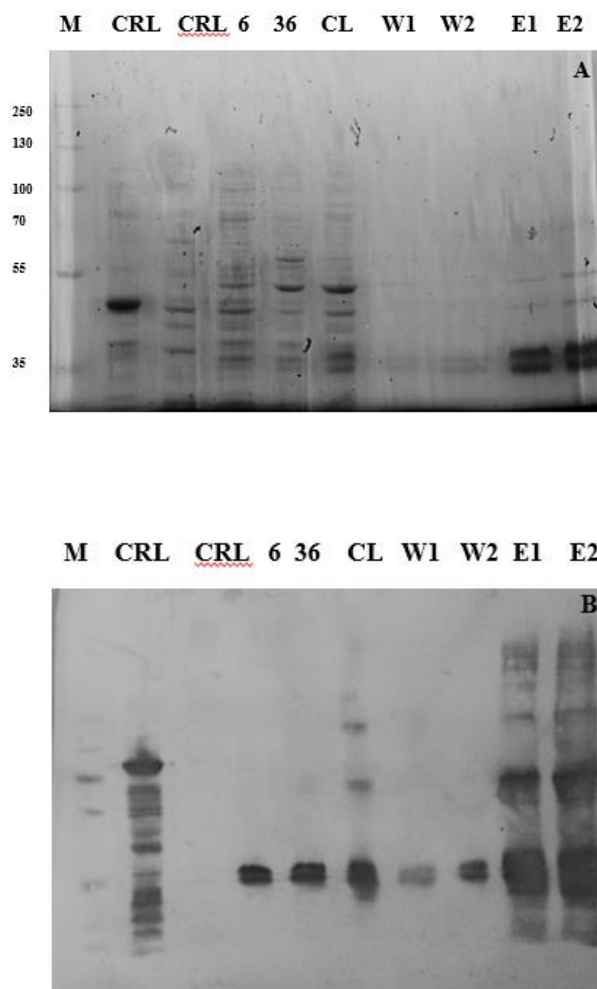


Figure 8: SDS-PAGE showing expression and purification of PflDH in 2YT medium at 25°C (A). Western blot showing purification of Recombinant PflDH (B). The PflDH protein was induced with IPTG at OD 0.4-0.6 and the samples were analyzed on 12% reducing SDS-PAGE gels, stained with Coomassie Brilliant Blue R-250. Panel A lane M: molecular weight marker, lane CRL: DNA ligase (positive control), lane CRL: BL21(negative control) lane 6: 6hr, lane 36: 36hrs (Time expression profile), lane CL: crude lysate, lane FT: unbound protein, lane W1: wash1, lane W2: wash 2, lane E1: elusion1, lane E2: elusion 2 (purified). Panel B Lane M: molecular weight marker, lane CR: crude lysate, lane FT: flow through, lane W1: wash 1, lane W2: wash 2, lane E1: elution 1, lane E2: elution 2. Lane M represents a molecular marker in kilodalton (kDa) used for sizing recombinant PflDH. Lane E1 and E2 in both panel (A & B) represents a successfully

purified PflDH protein sized 34.9kDa. Recombinant PflDH was not obtained as a single band as expected for purification but rather multiple bands. Multiple bands were also observed in other studies where they obtained two monomeric proteins of sizes 36 kDa and 33 kDa, a 75 kDa dimer and a 150 kDa tetramer (Sementa Khuzwayo Biochemistry, 2019). According to these studies this is the case because the sequence of PflDH contains an internal methionine at position 19, so this results in a product of two sizes of protein a 36 kDa full PflDH protein and a truncated 32 kDa (Sementa Khuzwayo Biochemistry, 2019).

4.2 Interaction Studies: Fourier transform infrared (FTIR) analysis and Ultraviolet-visible spectroscopy (UV-Vis)

Fourier transform infrared (FTIR) analysis and Ultraviolet-visible spectroscopy (UV-Vis) were used to conduct interaction studies to observe PflDH interaction with the investigated compounds. The spectra in figure 9 shows a highest absorbance reading for the PflDH only curve compared to PflDH + compound. If tyrosine residues are exposure, that can affect the binding of the protein to bioactive compounds, and in this case the absorbance should be higher for the spectra of PflDH only as all tyrosine residues are unoccupied as the compounds are absence (Opoku et al., 2019).

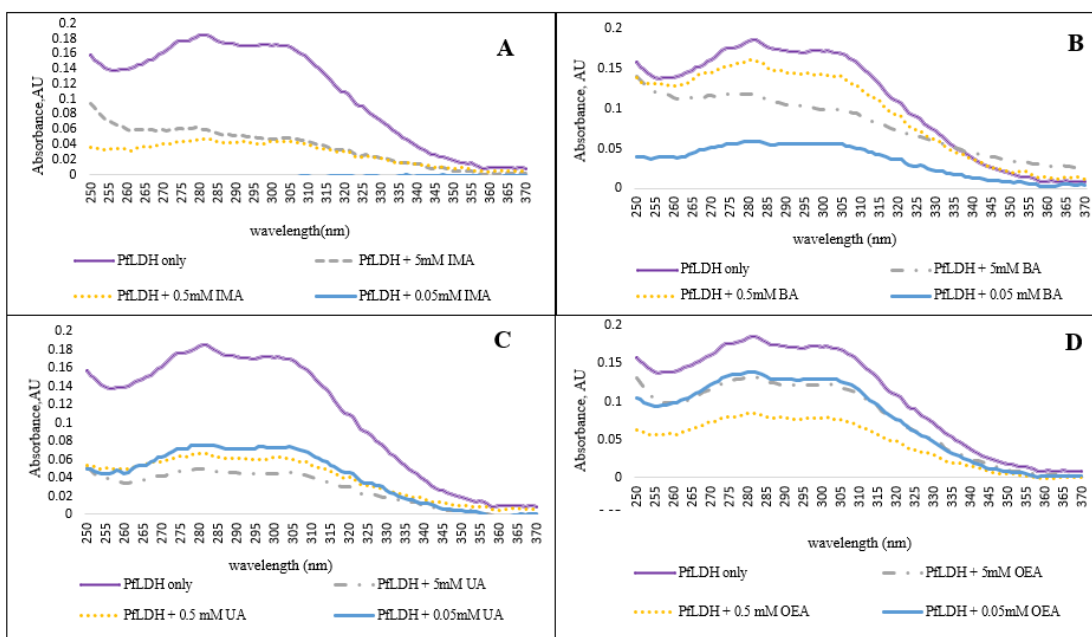


Figure 9: Uv-vis absorption spectra of PfLDH in the presence of Iso-mukaadial acetate IMA(A), Betulinic acid BA (B), Ursolic acid (C) and Oleanolic acid (D).

It can also be observed that the absorbance for PfLDH + Compounds (all four investigated compounds) are lower when compared to that of PfLDH only (Figure 9), this were expected results as in the presence of a compound the absorbance values are lower as fewer tyrosine residues are exposed (Opoku et al., 2019). In a presence of 5 mM Betulinic acid the absorbance values are lower compared to 0.5 mM Betulinic acid, this is an expected results because a highest compound concentration is expected to illustrate a lower absorbance than lower concentration. (Opoku et al., 2019). Although this was not a case for all the investigated compounds as 5 mM IMA had a higher absorbance value when compared to the other two lower concentration. These results provide evidence that BA, UA and OEA compound directly interact with PfLDH in a dose-dependent manner. Therefore, from these results it can be said that the structural conformational change was induced resulting in an interaction of the compounds with the aromatic side chains of PfLDH.

The interaction of IMA, BA, UA and OEA toward PfLDH were investigated using the FTIR vibration spectroscopy which provides information about the secondary structure content of proteins (Ohi, 2009).

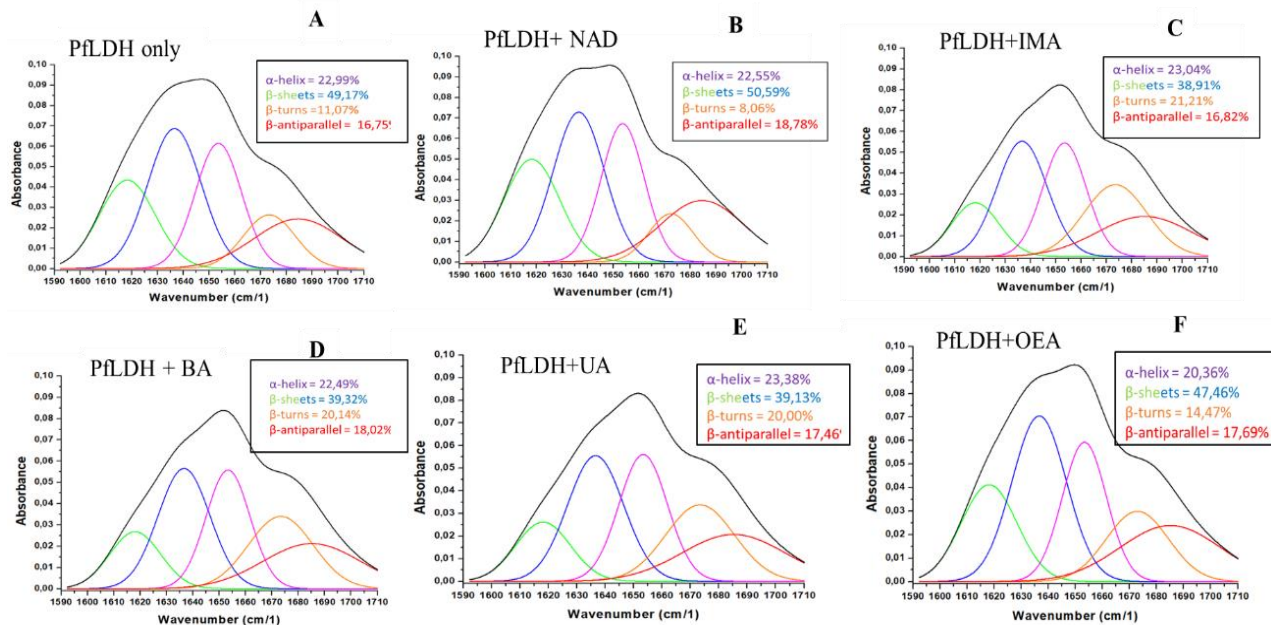


Figure 10: FTIR spectra of PflDH-compound interaction. The graphs show FTIR analysis for PflDH only, PflDH-1incubated with 5 mM NAD, PflDH incubated with 5 mM iso-mukaadial acetate ,5 mM Betulinic acetate, 5 mM Ursolic acid and 5mM Oleanolic Acid. Spectrum images labelled as fitted curve of amide band I at 1600–1700 cm^{-1} (A, B, C, D, E, and F).

An increase in α - helix percentages from 22.99% in the unbound PflDH to 23.04% with IMA and 23.38% with UA depicts structural change. This however was not the case for BA, OEA and NAD (a compound known to bind to PflDH) as the α - helix percentages there decreased from 22.99% to 22.49%, 20.36% and 22.55% respectively (figure 10). According to the t-test performed by GraphPad Prism these results were statistically difference as the p value obtained (0.00000003) was less than 0.05. The percentage increase (in IMA) indicates that PflDH conformational change was induced by IMA through the destabilized hydrogen bonds between the polypeptide strand (Salomane et al., 2021). This corresponds to the results obtained in a study done by Salomane et al., 2021 where it was noted that there was an increase in α - helix percentages from 21% in unbound PflHsp70-1 to 23% with Polymyxin B (PMB), 28% with IMA and 25% with Ursolic acetate (UAA).

4.3 Thermal stability assay

This assay monitored the thermal unfolding of PflLDH and presented the temperature at which the PflLDH was stable and temperature where it was denatured (Southard, n.d.). Figure 11 demonstrates increase in fluorescence as the temperature increases till it reaches a maximum temperature than starts decreasing. This sharp increase in fluorescence depicts unfolding of a PflLDH protein and binding of a dye, which expose the hydrophobic region of the unfolding protein (Southard, n.d.).

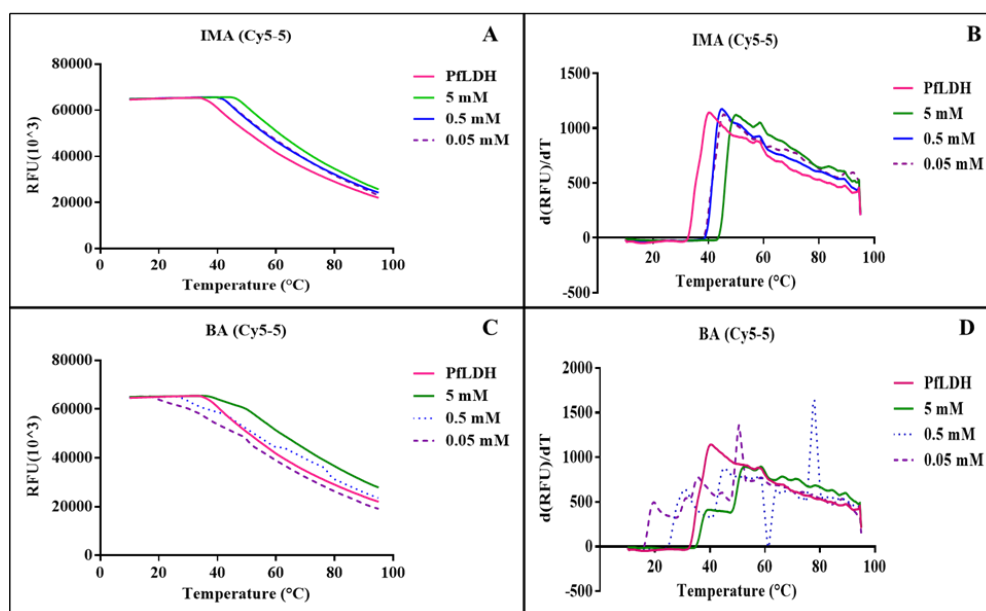


Figure 11: Thermal shift assay using cy5-5 environmentally sensitive fluorophores to check PflLDH stability in the presence of a compound.

This shows a successful protein thermal stability and increased melting temperature of PflLDH interacted with the two compounds BA and IMA. Other studies have shown that when a protein binds to a ligand, the folded state often becomes more stable, and T_m becomes affected by ligand concentration as well as binding affinity. Protein stability mainly characterizes the functionality or biological activity of the protein. Knowing the stability, or the melting temperature of the protein investigated is essential because the increase of temperature destabilized the protein by disrupting

covalent bonds, thus potentially altering biological activity of PfLDH meaning the protein loss its function. Most proteins' stability diminishes with increasing temperature (as see in this figure, at very high temperature the fluorescence starts to decrease). The investigated protein has the melting temperature between 30 °C and 35 °C (B and D), and PfLDH interacted with the highest concentration of BA or IMA showed increment of melting temperature. Thus, BA and IMA conferred protection to the protein and premature protein aggregation. Low concentrations of both compounds possibly altered the protein secondary structure by reducing alpha-helix and beta-sheet structure leading to a partial protein destabilization. An increase in T_m indicates stabilization and reflects compound binding and the effect of ligand binding on protein is concentration dependent. For some proteins, an increase in the concentration of ligand leads to multiple denaturation transitions or help further stabilize a ligand- binding domain that denatures at low temperature. (Senisterra et al., 2012). The melting temperature was calculated from the melt curve, which was generated from the protein thermal shift assay where changes in T_m was correlated to changes in protein stability or compound binding(Note, n.d.).

4.4 Molecular docking

Below is a table representing docking scores, type of interaction, distance, and binding affinity between PfLDH and the four investigated compounds (IMA, BA, UA, OEA) with the standard chloroquine. It also shows 2D and 3D figures representing the interaction of the compounds with the PfLDH protein.

Table 2: Docking scores (kcal/mol) with respective binding affinities and types of protein-ligand interactions including distance for the binding mode of Iso-makaadial acetate, Betulinic acid, Ursolic acid, Oleanolic acid and Chloroquine ligands with PfLDH.

Compound	Interaction	Distance	Docking score	Binding affinity
1 Betulinic acid	H-acceptor	2.97	-0.6	-5.7
2 Iso-mukaadial acetate	H-acceptor	3.11	-0.7	-5.6

3. Oleanolic Acid	H-donor	3.76	-0.5	-5.5
	H-acceptor	3.43	-0.9	
	H-acceptor	3.62	-5.4	
	H-acceptor	2.92	-13.9	
	Ionic	3.62	-1.5	
	Ionic	2.92	-5.1	
4. Ursolic acid	H-acceptor	3.33	-1.7	-5.9
	H-acceptor	2.87	-1.6	
	H-acceptor	3.59	-0.8	
5 chloroquine	H-donor	3.33	-0.8	-6.9
	H-donor	3.23	-1.4	
	H-donor	2.86	-11.7	
	H-donor	3.29	-1.4	
	Ionic	2.86	-5.5	
	ionic	3.29	-2.8	

Silico studies were done by performing a molecular docking analysis of IMA, BA, UA, and OEA (investigated compounds) and standard drug chloroquine with *Plasmodium falciparum* with the aim of investigating where these compounds bind on the *Plasmodium falciparum* lactate dehydrogenase crystal protein structure. Upon the completion of each docking approach, a maximum output of 5 distinct conformational clusters was calculated for each ligand. The molecule with lowest number for binding affinity (i.e., more negative) indicates highest binding affinity to the protein. The results showed that BA, IMA, UA, OEA and chloroquine has binding affinity of -5.7, -5.6, -5.9, -5.5 and -6.9 kcal/mol respectively (Table 2). When compared to the examined compounds, these binding affinities show that the known standard treatment (chloroquine) binds with higher affinity to PflDH. Chloroquine forms a three H-donor interaction with PflDH, having distance 3.33, 3.23, 2.86 and 3.29Å respectively with corresponding energy -0.8, -1.4, -11.7 and -1.4 kcal/mol and the residues involved in these H bonds are Asp 34, Gly 80

and Thr 78, Gly and Thr residues are also interacting residues for IMA and UA. It also had two ionic interactions distance 2.86 and 3.29Å with corresponding energy -5.5 and -2.8 kcal/mol. The interacting amino acid residues of PflLDH protein with chloroquine are Gly 80, Thr 78 and Asp 34 (Figure 12).

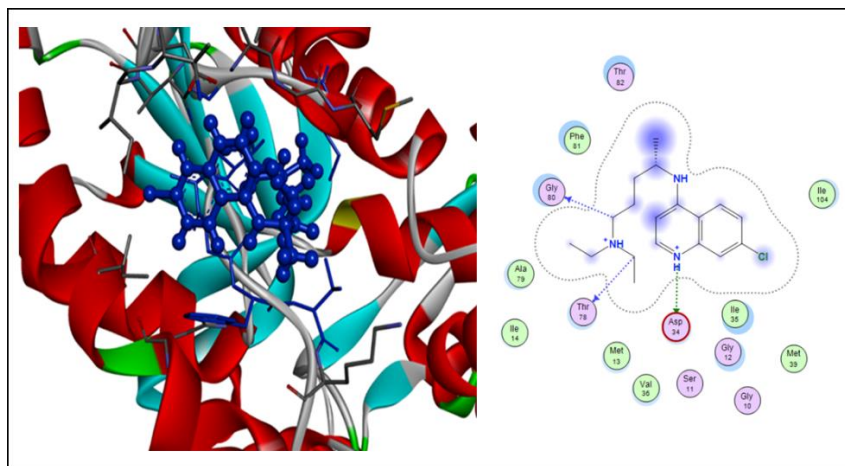


Figure 12: Three (3D) structure and two- dimensional (2D) structure of Chloroquine.

When comparing the four investigated compounds, Ursolic acid has a strong binding affinity of -5.9 kcal/mol to PflLDH when compared to the other three investigated compounds. UA has three H- acceptor interaction to PflLDH having distance of 3.33, 2.87, and 3.59Å with corresponding energy -1.7, -1.6, and -0.8 kcal/mol. The interacting amino acid residues of PflLDH protein with UA are Gly 80, Thr 82 and Ser 233 (Figure 13).

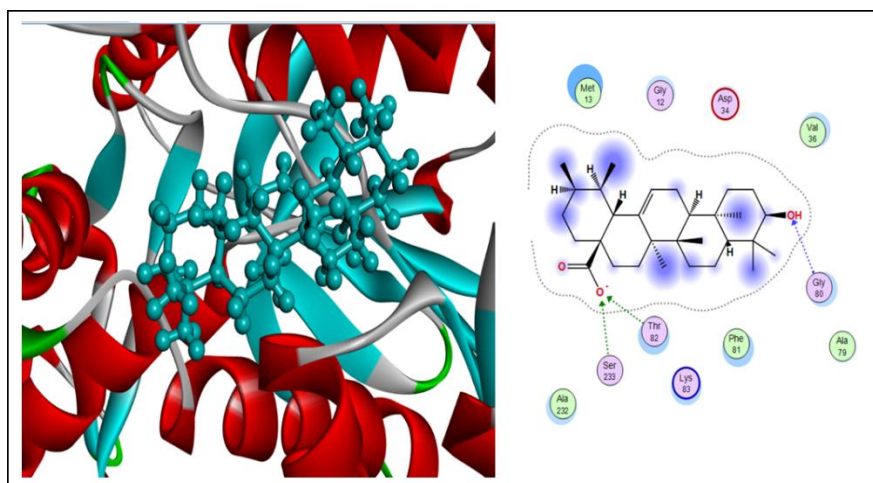


Figure 13: Three (3D) structure and two- dimensional (2D) structure of Ursolic acid

Although all the investigative compounds depicted binding affinity less than that of chloroquine, their binding affinities were close to that of chloroquine, particularly Ursolic acid as there is a small difference between the two compounds binding affinity. Iso-mukaadial acetate and Betulinic acid both form a hydrogen-acceptor bonds with PflLDH and the interacting amino acid residues of Gly12 for IMA with a distance of 3.11Å and energy of -0.7 kcal/mol, while the interacting amino acid residues for BA is Lys83 (Figure 14) with a distance of 2.97 and energy of -0.6 kcal/mol (Table 2).

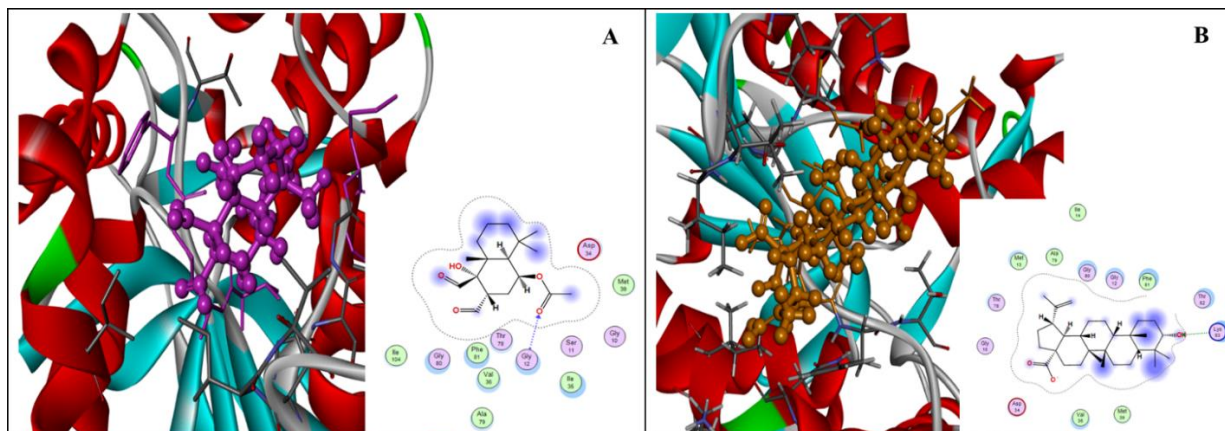


Figure 14: Three (3D) structure and two- dimensional (2D) structure of Iso-mukaadial acetate (A), Betulinic acid (B)

The binding energy illustrate the energy released due to the interaction of the ligand and protein. Chloroquine formed had the highest interactions: 6 interactions were formed with 3 amino acid residues Asp34, Thr78 and Gly80. Both BA and IMA had the same number of hydrogen bonds (1 H-bond (H-acceptor)).

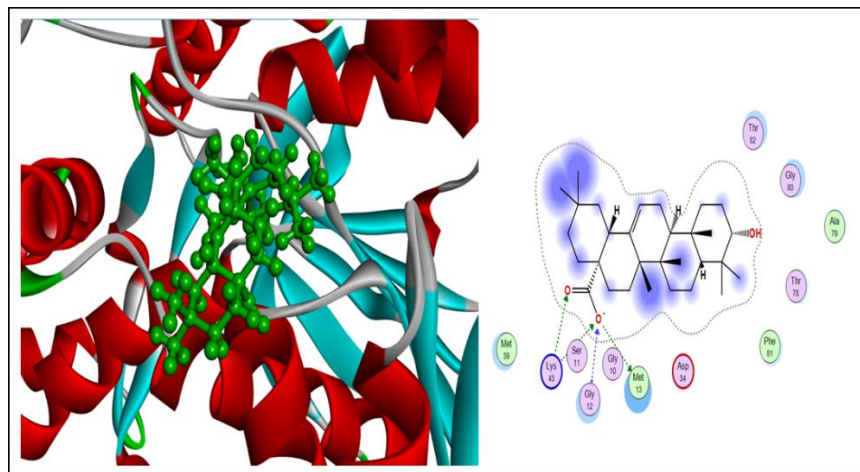


Figure 15: Three (3D) structure and two-dimensional (2D) structure of Oleanolic acid

UA and OEA also had three H-acceptor with one H-acceptor of UA having a smaller distance compared to the other three investigated compounds, suggesting how close the interaction of this compound and PfLDH is. This shorter distance might also explain why UA binds with a high affinity to PfLDH when compared to BA, IMA and OEA. A negative binding energy means the complex is bound spontaneously without consuming energy (i.e., more -ve BE means more stable) however if it is positive that means, one (ligand or compound) has to give that much amount of energy to form a complex. If BE is -ve then there will be the release of energy during the complex formation whereas a positive value means one must give that much energy to construct the complex. From the results UA might be a good inhibitor of PfLDH as it represented higher binding affinity to PfLDH these results also correlate with the inhibitory studies performed in this research as the compounds also showed good activity against asexual *P. falciparum* parasite given by their IC₅₀ values.

4.5 *Plasmodium falciparum* PfLDH inhibition studies

The inhibitory concentration (full dose response) of the two compounds (BA) which was determined using the SYBR Green I based assay on the NF54 (drug sensitive) strain of *P. falciparum* parasites showed that as the concentration of the compounds increased, the parasite proliferation decreased (figure 13). This shows that these compounds do inhibit the proliferation

of asexual *P. falciparum* parasite and it can be said that they possess anti-plasmodial activity (Dery et al., 2015) represented sigmoidal graphs showing the response of *P. falciparum* clinical isolates to artesunate, chloroquine and mefloquine. According to these graphs the relative effect (%) of these drugs decreased with the increasing concentration of artesunate, chloroquine and mefloquine, this meaning that although increasing the drug concentration does inhibit the proliferation of *P. falciparum* but very high concentration of these drugs does decrease their relative effectiveness (Dery et al., 2015). The main reason behind testing antimalarial activity for IMA and BA only is because these compounds have been found to be inhibitors of PfLDH (Opoku et al., 2019). We also took a further step to test antimalarial activity of the two extract (*Warburgia salutaris* (WB) and *Eucomis autumnalis* (EUM)) The IC₅₀ value of chloroquine (standard) obtained was 10±3 nM. The IC₅₀ values of compounds are considered highly active if they are in the same range or lower as compared to known antimalarial compounds. The two compounds IMA and BA which were screened for IC₅₀ values to show the overall activity against asexual *P. falciparum* parasite gave the follow results. BA and IMA showed IC₅₀ values of 1.27 and 1.03 µg/ml respectively against asexual *P. falciparum* parasite (Table 3), this representing good activity as these IC₅₀ values are less than 10µg/ml which is a classification criteria and represent good activity. The WB also showed good activity with IC₅₀ value of 2.14 µg/ml which is also less than 10µg/ml on the other hand the other extract showed IC₅₀ of 17.10 µg/ml showing moderate activity because it's between 10 and 20µg/ml. Out of all these tested compounds and extracts, IMA show good activity above all as it has the lowest IC₅₀ value (Maboane & Maboane, 2021). However, when QA the standard is compared to the two compounds (IMA & BA) and the two extract (WB & EUM) it has the lowest IC₅₀ value.

The table below represent the compound/ extract half maximum inhibitory concentration, which measured the compounds/ extract inhibition against *Plasmodium falciparum* parasite.

Table 3: IC₅₀ values for the screened compounds against asexual *Plasmodium falciparum* parasite, using SYBR Green I based assay.

Compound/ extract	NF54	
	IC ₅₀ (µg/ml)	+/- SEM/SD
BA	1.27	2.32
IMA	1.03	2.91
Chloroquine (QA)	0.01±3	
WB	2.41	2.63
EUM	17.10	3.27

The graphs below are a summary of dose response for the compounds and extracts tested. Curves are representative of biological repeats as indicated in each metrics.

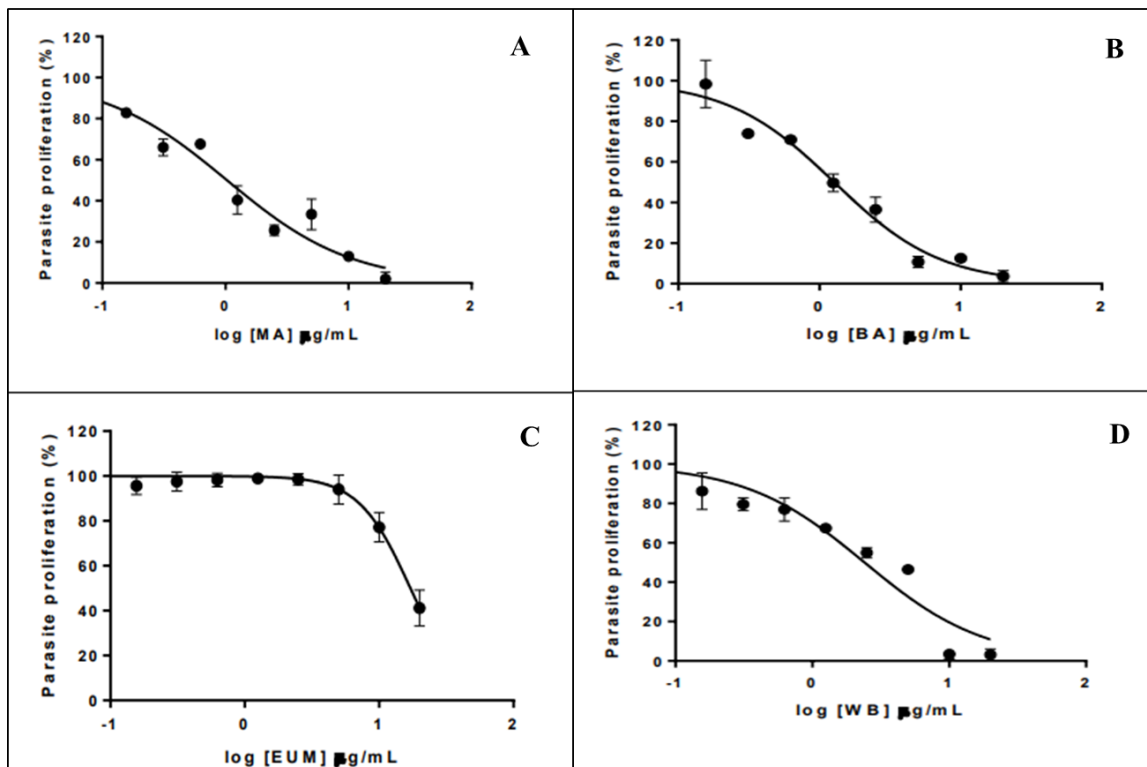


Figure 16: Dose response curves for the compounds and extracts tested for antimalarial activity. The different extract/ compound concentration influenced parasite proliferation. These panels shows that the log concentrations of the tested compounds/ extract are inversely proportional to the parasite proliferation. At very low concentration of compound/extract the parasite proliferation remains high but at very high concentrations the parasite proliferation decreased drastically.

CHAPTER 5: Conclusion

In this study the effect of four anti-plasmodium compounds IMA, BA, UA, and OEA towards inhibition of PfLDH was investigated. With the use of Ultraviolet-visible spectroscopy (UV-Vis), it was found that both BA and IMA do induce structural conformational change resulting in an interaction of the compound with the aromatic side chains of PfLDH. BA also directly interact with PfLDH in a dose-dependent manner, this was revealed by the highest concentration of BA 5mM having a lower absorbance compared to the smaller concentration of BA 0.5mM. However, IMA did show to interact with PfLDH but not in a dose-dependent manner as the highest IMA concentration 5mM did not show a lowest absorbance when compared to the other two smaller concentrations. With the use of FTIR spectroscopy an increase in α helix percentages depict structural change. Altogether *in vitro* and *in silico* studies show that the compounds (IMA and BA) interact with the PfLDH protein. Based on these findings, it is possible that these investigated compounds could be effective PfLDH inhibitors because they have binding affinities similar to the standard drug, chloroquine, and some of them have a more stable interaction than chloroquine due to their binding energy, especially UA it presented a higher binding affinity to PfLDH compared to the other investigated compounds. From this study we were able to observe the interaction between PfLDH and the four investigated compounds, furthermore, observing the ligand atoms responsible for the interaction. The limitations of the study were the omission of an enzymatic confirmation of the LDH activity conducted in the presence of the various compounds to validate its structural findings, and we could find a way around this is future by experimenting with different LDH activity to find the best suitable one for PfLDH protein. Another limitation is not being able to perform sequencing to conclude that the gene encoding PfLDH was successfully cloned in the PKK223 plasmid. Future perspectives include investigating the mechanism of action, in order to observe how these compounds, affect PfLDH.

References

- Ajmal Ali, M. (2020). Molecular docking and molecular dynamics simulation of anticancer active ligand '3,5,7,3',5'-pentahydroxy-flavanonol-3-O- α -L-rhamnopyranoside' from *Bauhinia strychnifolia* Craib to the cyclin-dependent protein kinase. *Journal of King Saud University - Science*, 32(1), 891–895.
- Alam, A., Neyaz, K., & Hasan, S. I. (2014). Exploiting Unique Structural and Functional Properties of Malarial Glycolytic Enzymes for Antimalarial Drug Development. 2014.
- Barat, L. M., & Bloland, P. B. (1997). Drug resistance among malaria and other parasites. *Infectious Disease Clinics of North America*, 11(4), 969–987.
- Capela, R., Moreira, R., & Lopes, F. (2019). An Overview of Drug Resistance in Protozoal Diseases.
- Dery, V., Duah, N. O., Ayanful-Torgby, R., Matrevi, S. A., Anto, F., & Quashie, N. B. (2015). An improved SYBR Green-1-based fluorescence method for the routine monitoring of *Plasmodium falciparum* resistance to anti-malarial drugs. *Malaria Journal*, 14(1), 1–6.
- Eugene, K. (2017). Recombinant expression and bioinformatic analysis of *Plasmodium falciparum* lactate dehydrogenase and heat shock protein 70-1 by Submitted in fulfilment of the academic requirements for the degree of Master of Science in Biochemistry School of Life Science.
- Fabricant, D. S., & Farnsworth, N. R. (2001). The Value of Plants Used in Traditional Medicine for Drug Discovery. *Environmental Health Perspectives*, 109(March), 69.
- Hyde, J. E. (2007). Drug-resistant malaria) an insight. 274, 4688–4698.
- K. Ambre, P., R. S. Pissurlenkar, R., S. Jagyasi, A., A. Fule, R., Khedkar, V., R. Barhate, C., Vivas, L., K. Tripathi, A., Sullivan, D., Birkinshaw, R., Leo Brady, R., Iyer, K., & C. Coutinho, E. (2013). Molecular Modeling Studies, Synthesis and Biological Evaluation of Novel *Plasmodium falciparum* Lactate Dehydrogenase (pLDH) Inhibitors. *Anti-Infective Agents*, 10(1), 55–71.
- Keiser, J., Singer, B. H., & Utzinger, J. (2005). Reducing the burden of malaria in different eco-epidemiological settings with environmental management: A systematic review. *Lancet*

Infectious Diseases, 5(11), 695–708.

- Lueangyangyuen, A., Senapin, S., Dong, H. T., Unajak, S., Wangkahart, E., & Khunrae, P. (2021). Expression and purification of S5196-272 and S6200-317 proteins from Tilapia Lake Virus (TiLV) and their potential use as vaccines. *Protein Expression and Purification*, 190(October 2021), 106013.
- Maboane, S., & Maboane, S. (2021). REPORT TO : Dr . Ofentse Pooe Block F3 - Room 04-025 Discipline of Biochemistry School of Life Science University of KwaZulu-Natal Westville campus , University Road P / Bag X54001 , Durban , 4000. 25–28.
- Mathema, V. B., & Na-bangchang, K. (2015). A brief review on biomarkers and proteomic approach for malaria. *Asian Pacific Journal of Tropical Medicine*, 8(4), 253–262.
- Mathema, V. B., & Na-Bangchang, K. (2015). A brief review on biomarkers and proteomic approach for malaria research. *Asian Pacific Journal of Tropical Medicine*, 8(4), 253–262.
- Nava, A., Shimabukuro, J. S., Chmura, A. A., Luiz, S., & Luz, B. (2017). The Impact of Global Environmental Changes on Infectious Disease Emergence with a Focus on Risks for Brazil. January 2018, 1–8.
- Note, A. (n.d.). Protein Thermal Shift technology Optimizing buffer conditions and high-throughput screening of ligand-protein binding.
- Nyaba, Z. N., Murambiwa, P., Opoku, A. R., Mukaratirwa, S., Shode, F. O., & Simelane, M. B. C. (2018). Isolation, characterization, and biological evaluation of a potent anti-malarial drimane sesquiterpene from *Warburgia salutaris* stem bark. *Malaria Journal*, 17(1).
- Opoku, F., Govender, P. P., Pooe, O. J., & Simelane, M. B. C. (2019). Evaluating iso-mukaadial acetate and ursolic acid acetate as plasmodium falciparum hypoxanthine-guanine-xanthine phosphoribosyltransferase inhibitors. *Biomolecules*, 9(12).
- Ouellette, M., & Ward, S. A. (2003). Drug resistance in parasites. In *Molecular Medical Parasitology*.
- Pierre, S., Fernand-n, T. F., Alexandre-michel, N. N., & Jean, M. (2011). Medicinal plants used in traditional treatment of malaria in Cameroon. 3(March), 104–117.

- Resistance, D. (2020). Antimalarial Drug Resistance and Novel Targets for Antimalarial Drug Discovery.
- Salomane, N., Poee, O. J., & Simelane, M. B. C. (2021). Iso-mukaadial acetate and ursolic acid acetate inhibit the chaperone activity of Plasmodium falciparum heat shock protein 70-1. *Cell Stress and Chaperones*, 26(4), 685–693.
- Sementa Khuzwayo Biochemistry, S. (2019). Recombinant Expression, Purification, Analysis and Immunization of Mice with Plasmodium yoelii Glyceraldehyde-3-Phosphate Dehydrogenase (rPyGAPDH) and Lactate Dehydrogenase (rPyLDH) and Evaluation of Protection against P. berghei.
- Shift, P. T., & Preparation, S. (n.d.). Protein Thermal Shift Assays Made Easy with Bio-Rad 's Family of CFX Real-Time PCR Detection Systems. 1–8.
- Southard, J. N. (n.d.). Protein Analysis Using Real-Time PCR Instrumentation : Incorporation in an integrated , inquiry-based project. 142–151.
- Tse, E. G., Korsik, M., & Todd, M. H. (2019). The past , present and future of anti - malarial medicines. *Malaria Journal*, 1–21.
- Valvona, C. J., Fillmore, H. L., Nunn, P. B., & Pilkington, G. J. (2015). The Regulation and Function of Lactate Dehydrogenase A : Therapeutic Potential in Brain Tumor. 1–15.
- Vaughan, K., Greenbaum, J., Blythe, M., Peters, B., & Sette, A. (2010). Meta-analysis of All Immune Epitope Data in the Flavivirus Genus : Inventory of Current Immune Epitope Data Status in the Context of Virus Immunity and Immunopathology. 23(3), 259–284.
- Wang, W. X., Cheung, Y. W., Dirkwager, R. M., Wong, W. C., Tanner, J. A., Li, H. W., & Wu, Y. (2017). Specific and sensitive detection of Plasmodium falciparum lactate dehydrogenase by DNA-scaffolded silver nanoclusters combined with an aptamer. *Analyst*, 142(5), 800–807.
- Willcox, M. L., & Bodeker, G. (2004). Clinical review Traditional herbal medicines for malaria. 329(November).

Appendices

This part shows information that was not represented either on the methodology or the results section.

Appendix A: Preparation of reagents

Tris for SDS- PAGE

1.5M Tris (PH 8.8): 18.15g of Tris, make up to 100ml with d-H₂O

0.5M Tris (PH 6.8): 6g of Tris, make up to 100ml with d-H₂O

10% Ammonium persulphate

1g of 10% APS then make up to 10ml with d-H₂O

100µg/ml Ampicillin

1g ampicillin then make up to ml with d-H₂O

Western blot buffer

3.03g of 25mM Tris, 14.4g of 192 mM glycine and 200ml of 20% methanol then make up to 1000ml

Tris buffered saline (TBS)

6.05g of 50mM Tris and 8.76g of 150mm of NaCl, make up with d-H₂O

TBS-Tween 20 (TBST)

1ml Tween 20 in 1L TBS

Coomassie Destain

400ml methanol and 70ml Glacial acetic acid make up with water to 1L

Coomassie stain

1.25g Coomassie in 500ml destain

1mM IPTG

Filter sterilize 2.383g of IPTG and make up to 10ml with d-H₂O

Appendix B: Protein expression optimization

Table 1: Different types of media used with the reagent ingredient to prepare them

Media	Ingredients
Lysogeny media	1% w/v tryptone, 0.03 % w/v sodium chloride and 0.5% w/v yeast extract
Terrific media	yeast extract, tryptone, glycerol and phosphate buffer [0.17M KH ₂ PO ₄ , 0.72 K ₂ HPO ₄]
YEP media	yeast extract, peptone, NaCl
2YT media	yeast extract, tryptone, NaCl

Table 2: Optimization of type of media and temperature

Media	Temperature
Lysogeny media	37°C 30°C
Terrific media	37°C
YEP media	37°C
2YT media	37°C
2YT media	25°C

Expression was optimized by using different media, where protein was first expressed in lysogeny media 37°C then at 30°C. The second media which was used for expression was terrific media at 37°C, follow by YEP media at 37°C, then lastly 2YT media at 37°C then at a temperature 25°C which was the final media and temperature chosen as the PflDH protein showed to be expressed better in this media.

Appendix C: Double digestion

Table 3: Reagents and their measurements in each of the four micro-centrifuge tubes for double digestion.

	Uncut (Control) (μ l)	Cut (BamHI) (μ l)	Cut (HindIII) (μ l)	Cut (BamHI & HindIII) (μ l)
DNA	2	2	2	2
Buffer	2	2	2	2
Distilled water	16	15	15	14
Enzyme	-	1	1	1+1 (both enzyme)

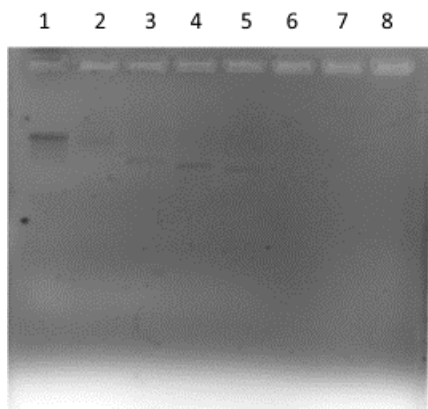


Figure 1: 1% Agarose gel electrophoresis for double digestion. Double digestion was performed with restriction enzyme BamHI and HindIII to confirm cloning of the gene in plasmid pkk223. Lane 1: lambda DNA, lane 2: uncut plasmid, lane 3: plasmid cut with BamHI, lane 4: plasmid cut with HindIII, lane 5: plasmid cut with HindIII and BamHI.

Appendix D:

Table 4: Colony PCR cycling conditions for amplifying recombinant PflDH gene

PCR cycles	Steps	Temperature	Duration
	Initial denaturation	95°C	3 min
Cycles (30×)	Denaturation	94°C	30 sec

Annealing	49.0°C	1 min
Extension	68.0°C	1 min

Appendix E: Preparations of Sodium dodecyl sulphate polyacrylamide gel electrophoresis (SDS-PAGE)

SDS-PAGE gel was prepared as described in (Table) and poured between two glass plates: 81.5 mm x 101.5 mm and 72.5 mm x 101.5 mm. The running gel was overlaid with distilled water and the water was removed once the running gel had polymerized. Stacking gel was added and 10 well combs was inserted. Afterwards, the gel plates were assembled in the casting gasket(Sementha Khuzwayo Biochemistry, 2019)

Table 5: Reagents and recipe for preparation of running and stacking gel

Reagents	Running gel	Stacking gel
d-H₂O	3.2ml	2.975ml
Bis-Acrylamide	4ml	0.67ml
1.5 Tris (pH 8.8)	2.6ml	-
0.5 Tris (pH 6.8)	-	1.25ml
20% SDS	50µl	25µl
10% APS	100µl	50µl
Temed	10µl	5µl

The sample preparation was done as follows: 20µl sample reducing treatment buffer and 80 µl of protein sample and mixed by pipetting up and down then boiled for 15 min. Standard molecular weight marker was run along with the samples to estimate the molecular weights of the protein.

Electrophoresis was performed using a Bio-Rad system at 120V with tank buffer for 1 h and the gels were stained with Coomassie brilliant blue R- 250 and then destained.

Appendix F: Recombinant PflLDH expression and purification using difference media and variety of temperatures

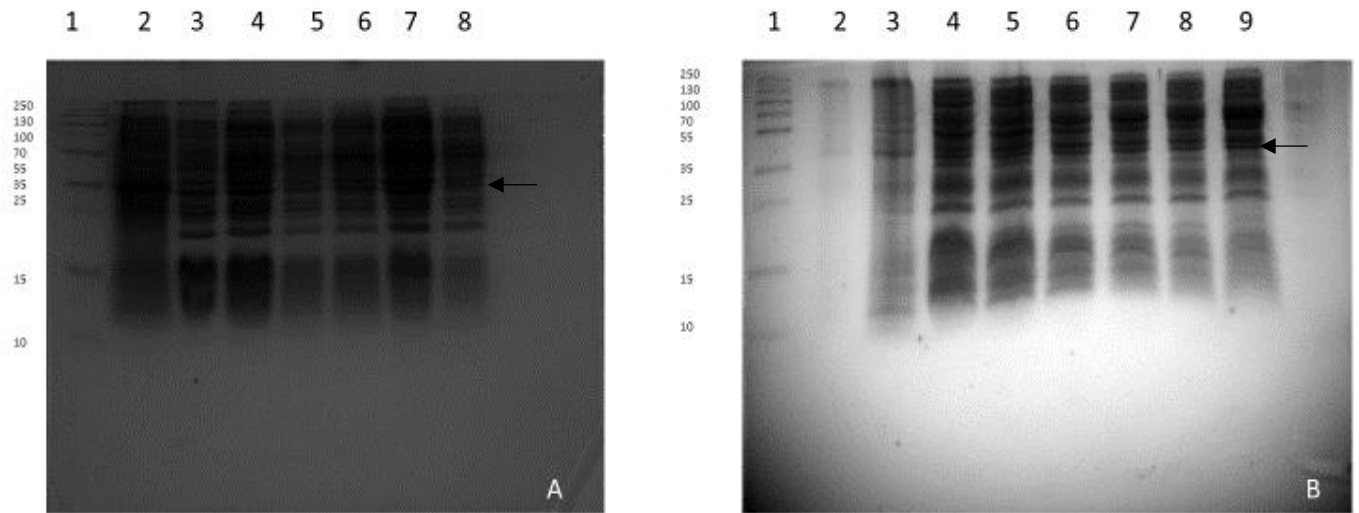


Figure 2: SDS-PAGE of an expression of PflLDH in Lysogeny Broth (LB) and at 37°C. Recombinant PflLDH was expressed at 37°C in LB (panel A) and was uninduced, was also expressed at 37°C in LB (panel B) and was induced with IPTG. The samples were analyzed on 15% reducing SDS-PAGE gels, stained with Coomassie Brilliant Blue R-250. Panel A lane 1: molecular weight marker, lane 2: BL21 (negative control), lane 3: 0hr, lane 4: 1hr, lane 5: 2hrs, lane 6: 3hrs, lane 7: 6hrs, lane 8: 24hrs (Time expression profile). Panel B Lane 1: molecular weight marker, lane 2 nothing (spill), lane 3: BL21, lane 4: 0hr, lane 5: 1hr, lane 6: 2hrs, lane 7: 3hrs, lane 8: 4hrs, lane 9: 24 hrs (Time expression profile). The experiment was repeated two times, an example experiment is shown. The arrow shows the expected size (34 KDa) of PflLDH protein.

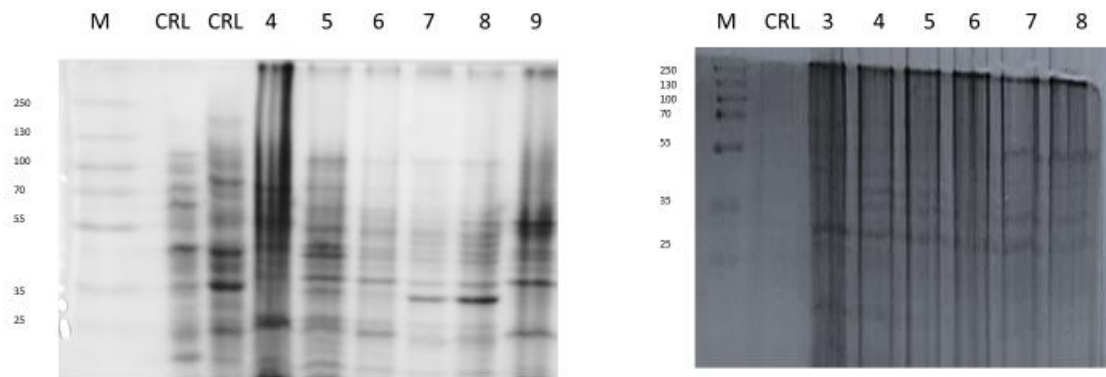


Figure 3: SDS-PAGE of an expression of PflDH in Lysogeny Broth (LB) and at 30°C. Recombinant PflDH was expressed at 30°C in LB (panel A) and was uninduced, was also expressed at 30°C in LB (panel B) and was induced with IPTG. The samples were analyzed on 15% reducing SDS-PAGE gels, stained with Coomassie Brilliant Blue R-250. Panel A lane 1: molecular weight marker, lane 2: BL21 (negative control), lane 3: (positive control), lane 4: 0hr, lane 5: 1hr, lane 6: 2hrs, lane 7: 3hrs, lane 8:4hrs, lane 9: 24hrs (Time expression profile). Panel B Lane 1: molecular weight marker, lane 2: (positive control), lane 3: 0hr, lane 4: 1hr, lane 5: 2hrs, lane 6: 3hrs, lane 7: 4hrs, lane 8: 24hrs (e expression profile). The arrow shows the expected size (34 KDa) of PflDH protein.

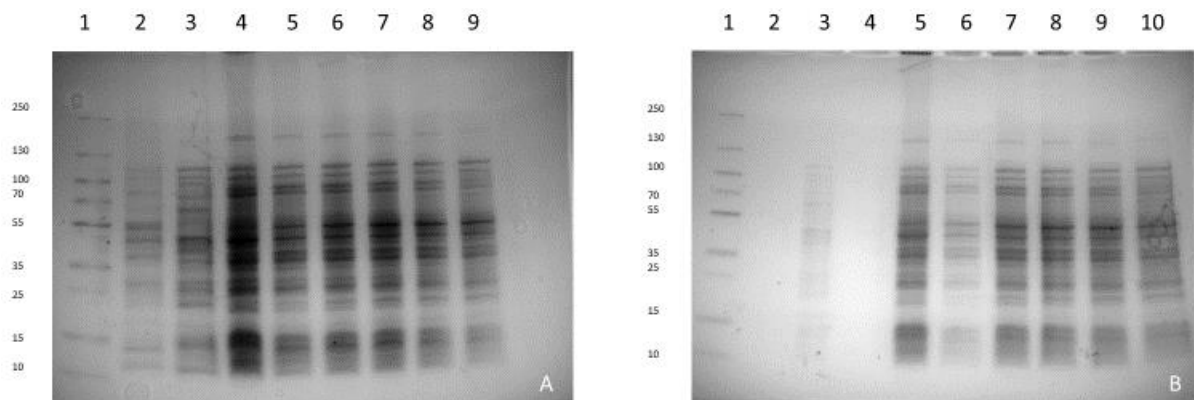


Figure 4: SDS-PAGE of an expression of PflDH in Terrific Broth (TB) and at 37°C. Recombinant PflDH was expressed at 37°C in TB (panel A) and was uninduced, was also expressed at 37°C in TB (panel B) and was induced with IPTG. The samples were analyzed on 15% reducing SDS-PAGE gels, stained with Coomassie Brilliant Blue R-250. Panel A lane 1:

molecular weight marker, lane 2: positive control, lane 3: BL21 (negative control), lane 4: 0hr, lane 5: 1hr, lane 6: 2hrs, lane 7: 3hrs, lane 8:4hrs, lane 9: 24hrs (Time expression profile). Panel B Lane 1: molecular weight marker, lane 2: (positive control), lane 3: BL21 (negative control), lane 4: nothing, lane 5: 0hr, lane 6: 1hr, lane 7: 2hrs, lane 8: 3hrs, lane 9: 4hrs, lane 10: 24hrs (Time expression profile). The arrow shows the expected size (34 KDa) of PflDH protein.

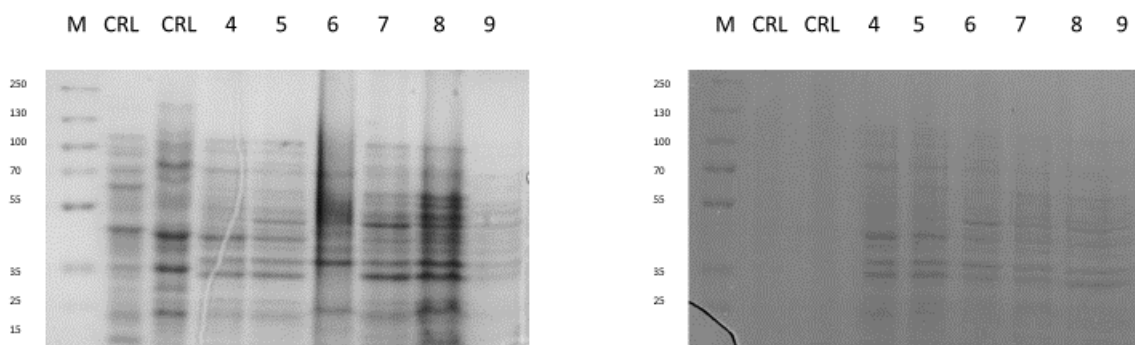


Figure 5: SDS-PAGE of an expression of PflDH in YEP medium at 37°C. Recombinant PflDH was expressed at 37°C in YEP (panel A) and was uninduced, was also expressed at 37°C in YEP (panel B) and was induced with IPTG. The samples were analyzed on 15% reducing SDS-PAGE gels, stained with Coomassie Brilliant Blue R-250. Panel A lane 1: molecular weight marker, lane 2: BL21(negative control), lane 3: (positive control), lane 4: 0hr, lane 5: 1hr, lane 6: 2hrs, lane 7: 3hrs, lane 8:4hrs, lane 9: 24hrs (Time expression profile). Panel B Lane 1: molecular weight marker, lane 2: BL21(negative control), lane 3: (positive control), lane 4: 0 hr, lane 5: 1hr, lane 6: 2hrs, lane 7: 3hrs, lane 8: 4hrs, lane 9: 24hrs (Time expression profile). The arrow shows the expected size (34 KDa) of PflDH protein.

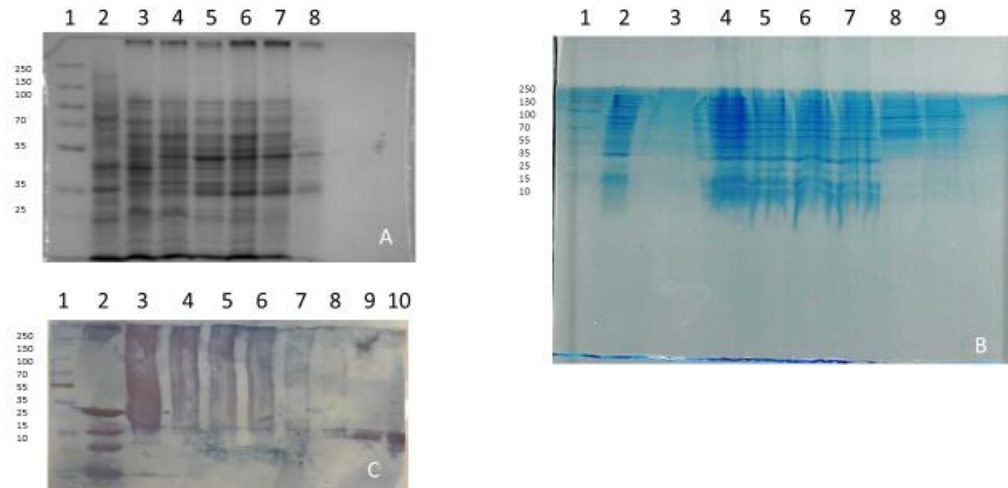


Figure 6: SDS-PAGE and blot of an expression of PflLDH in 2YT medium at 37°C. Recombinant PflLDH was expressed at 37°C in 2YT (panel A) and was uninduced, was also expressed at 37°C in 2YT (panel B) and was induced with IPTG. The samples were analyzed on 15% reducing SDS-PAGE gels, stained with Coomassie Brilliant Blue R-250. Panel A lane 1: molecular weight marker, lane 2: (positive control), lane 3: 0hr, lane 4: 1hr, lane 5: 2hrs, lane 6: 3hrs, lane 7:4hrs, lane 8: 24hrs (Time expression profile). Panel B Lane 1: molecular weight marker, lane 2: BL21(negative control), lane 3: (positive control), lane 4: 0 hr, lane 5: 1hr, lane 6: 2hrs, lane 7: 3hrs, lane 8: 4hrs, lane 9: 24hrs (Time expression profile). Panel C shows a blot for protein expression confirmation, lane 1: molecular weight marker, lane 2: (positive control), lane 3: TB 0hr, lane 4: TB 1hr, lane 5: TB 2hrs, lane 6: TB 3hrs, lane 7: TB 4hrs, lane 8: TB 24hrs, lane 9: YEP, uninduced 3hrs, lane 10: 2YT uninduced 3hrs. The arrow shows the expected size (34 KDa) of PflLDH protein.

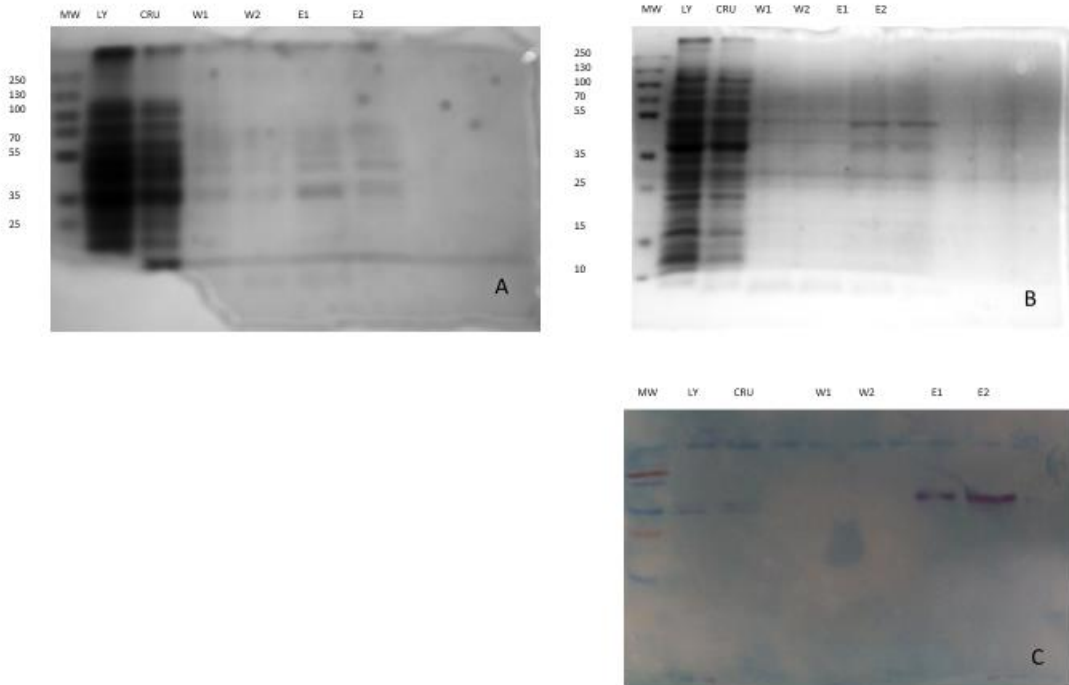


Figure 7: SDS-PAGE and western blot of affinity purification of recombinant PFLDH. Recombinant PFLDH was expressed in *E. coli* BL21 (DE3) cells grown in four different media and was grown in 2YT for a large scale in order to perform affinity purification with a nickel affinity matrix. Samples were analysed on a 15% SDS-PAGE gel (Panel A and B) and Western blot (Panel C). Panel A is purification with 100mM imidazole lane 1: molecular weight marker; lanes 2: lysate, lane 3: crude lysate, lane 4: wash 1, lane 5: wash 2, lane 6: elution 1, lane 7: elution 2. Panel B is purification with 500mM imidazole lane 1: molecular weight marker, lane 2: lysate, lane 3: crude lysate, lane 5: wash 1, lane 6: wash 2, lane 8: elution 1, lane 9: elution 2. The gel was stained with Coomassie brilliant blue R- 250. The western blot was probed with anti-Histag antibody.

Appendix G: Bradford assay for determination of protein concentration

Table 6: Bovine serum albumin standard concentrations and corresponding absorbance values

BSA standard concentrations ($\mu\text{g/ml}$)	Absorbance (Abs 595nm)
0	0
6.25	0.0016
12.5	0.0458
25	0.0465
50	0.0768
100	0.1544

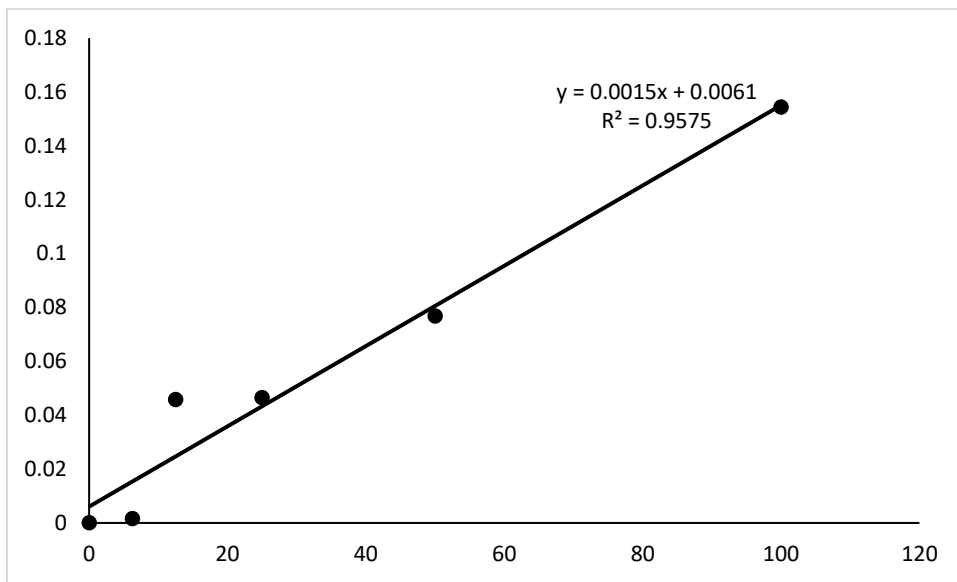


Figure 8: Bradford standard curve for protein concentration determination

Bovine serum albumin (BSA) standard concentration ranging from 0 to 100 $\mu\text{g/ml}$ were prepared and absorbance was read at wavelength of 595nm using a Bio-Rad spectrophotometer. The $R^2 = 0.9575$ and the linear equation: $y=0.0015x + 0.0061$ was used to calculate the protein concentration.